been approved for treatment of AS in Europe, the number of AS patients undergoing infliximab therapy will presumably increase. Therefore, in addition to the known biological adverse events of infliximab, physicians should evaluate all AS patients with severe symptoms for an underlying pseudoarthrosis.

References

[1] Braun J, Sieper J. Biological therapies in the spondyloarthritides—the current state. Rheumatology (Oxford) 2004;43:1072–84.

[2] Braun J, Brandt J, Listing J, et al. Long-term efficacy and safety of infliximab in the treatment of ankylosing spondylitis: an open, observational, extension study of a three-month, randomized, placebo-controlled trial. Arthritis Rheum 2003;48:2224–33.

[3] Temekonidis TI, Alamanos Y, Nikas SN, et al. Infliximab therapy in the patients with ankylosing spondylitis: an open label 12 month study. Ann Rheum Dis 2003;62:1218–20.

[4] Andersson O. Röntgenbilder vid spondylarthritis ankylopoetica. Nord Med 1937;14:2000–2.

[5] Wholey MH, Pugh DG, Bickel WH. Localized destructive lesions in rheumatoid spondylitis. Radiology 1960;74:54–6.

[6] Kaneficld DG, Mullins BP, Frechafer AA, Furey JG, Horenstein S, Chamberlin WB. Destructive lesions of the spine in rheumatoid ankylosing spondylitis. J Bone Joint Surg [Am] 1969;51-A:1369–75.

[7] Cawley MID, Chalmers TM, Kellgren JH, Ball J. Destructive lesions of vertebral bodies in ankylosing spondylitis. Ann Rheum Dis 1972;31:345–58.

[8] Yau ACMC, Chan RNW. Stress fracture of the fused lumbodorsal spine in ankylosing spondylitis. A report of three cases. J Bone Joint Surg [Br] 1974;56-B:681–7.

[9] Sutherland RIL, Matheson D. Inflammatory involvement of vertebrae in ankylosing spondylitis. J Rheumatol 1975;2:296–302.

[10] Dihlmann W, Delling G. Discovertebral destructive lesions (so called Andersson lesions) associated with ankylosing spondylitis. Skeletal Radiol 1978;3:10–6.

[11] Martel W. Spinal pseudoarthrosis: a complication of ankylosing spondylitis. Arthritis Rheum 1978;21:485–90.

[12] Resnick D, Niwayama G. Discovertebral destruction in a man with chronic back problem. Invest Radiol 1981;16:89–94.

[13] Weinstein PR, Karpman RR, Gall EP, Pitt M. Spinal cord injury, spinal fracture, and spinal stenosis in ankylosing spondylitis. J Neurosurg 1982;57:609–16.

[14] Hunter T, Dubo HIC. Spinal fractures complicating ankylosing spondylitis: a long-term followup study. Arthritis Rheum 1983;26:751–9.

[15] Wise CM, Irby WR. Spondylodiscitis in ankylosing spondylitis: variable presentations. J Rheumatol 1983;10:1004–6.

[16] Chan FL, Ho FK, Fang D, Hsu LC, Leong JC, Ngan H. Spinal pseudoarthrosis complicating ankylosing spondylitis. Acta Radiol 1987; 28:383–8.

[17] Fang D, Leong JC, Ho EK, Chan FL, Chow SP. Spinal pseudoarthrosis in ankylosing spondylitis: clinicopathological correlation and the results of anterior spinal fusion. J Bone Joint Surg [Br] 1988;70-B: 443–7.

[18] Hunter T. The spinal complications of ankylosing spondylitis. Semin Arthritis Rheum 1989;19:172–82.

[19] Agarwal AK, Reidbord HE, Kraus DR, Eisenbeis CH Jr. Variable histopathology of discovertebral lesion (spondylodiscitis) of ankylosing spondylitis. Clin Exp Rheumatol 1990;8:67–9.

[20] Peh WCG, Luk KDK. Pseudoarthrosis in ankylosing spondylitis. Ann Rheum Dis 1994;53:206–10.

[21] Pettersson T, Laasonen L, Leirisalo-Repo M, Tervahartiala P. Spinal pseudoarthrosis complicating ankylosing spondylitis: a report of two patients. Br J Rheumatol 1996;34:1319–23.

[22] Rasker JJ, Prevo RL, Lanting PJH. Spondylodiscitis in ankylosing spondylitis: inflammation or trauma? Scand J Rheumatol 1996;25: 52–7.

THE JOURNAL OF BIOLOGICAL CHEMISTRY VOL. 281, NO. 41, pp. 31079–31092, October 13, 2006

Oxygen Tension Regulates Chondrocyte Differentiation and Function during Endochondral Ossification*

Received for publication, March 10, 2006, and in revised form, July 13, 2006 Published, JBC Papers in Press, August 11, 2006, DOI 10.1074/jbc.M602296200

Makoto Hirao‡, Noriyuki Tamai‡, Noriyuki Tsumaki‡, Hideki Yoshikawa‡, and Akira Myoui‡§1

From the ‡Department of Orthopaedics, Osaka University Graduate School of Medicine, 2-2 Yamadoaka, Suita, Osaka 565-0871, Japan and §Medical Center for Translational Research, Osaka University Hospital, 2-15 Yamadaoka, Suita, Osaka 565-0871, Japan

Cartilage functions at a lower oxygen tension than most other tissues. To determine the role of oxygen tension in chondrocyte differentiation and function, we investigated the influence of oxygen tension in the pluripotent mesenchymal cell line C3H10T1/2 and 14.5E mice embryo forelimb organ culture. 10T1/2 cells and embryo forelimbs were cultured under normoxia (20% O_2) or hypoxia (5% O_2) in the presence of recombinant human bone morphogenetic protein 2. To elucidate the mechanism by which oxygen tension influences chondrocyte differentiation, the Smad pathway was examined using Smad6 overexpression adenovirus and Smad6 transgenic mice embryo forelimbs. The p38 MAPK pathway was examined using dominant-negative MKK3 and FR167653, a specific p38 MAPK inhibitor. The transcriptional activities of Sox9 and Runx2 were also investigated. Hypoxia promoted bone morphogenetic protein 2-induced glycosaminoglycan production and suppressed alkaline phosphatase activity and mineralization of C3H10T1/2. Thus, hypoxia promoted chondrocytic commitment rather than osteoblastic differentiation. In the mice embryo forelimb organ culture, hypoxia increased cartilaginous matrix synthesis. These effects were primarily mediated by p38 MAPK activation, independent of Sox9. Hypoxia inhibited *Col10a1* (type X collagen α1) expression via down-regulation of Runx2 activity by Smad suppression and histone deacetylase 4 activation. In conclusion, hypoxia promotes chondrocytic differentiation and cartilage matrix synthesis and suppresses terminal chondrocyte differentiation. These hypoxia-induced phenomena may act on chondrocytes to enhance and preserve their phenotype and function during chondrocyte differentiation and endochondral ossification.

A number of pathophysiological findings suggest that a correlation exists between hypoxia and chondrogenesis. For example, articular cartilage is an avascular tissue that functions at an oxygen tension that is lower than that of most other tissues. Articular cartilage derives both its nutrition and oxygen supply by diffusion from the synovial fluid and the subchondral bone. It has been estimated that articular chondrocytes in the deepest layers may have access to no more than 1–6% O_2 (1–6). Furthermore, although the majority of mammalian cells derive their energy by using oxygen for mitochondrial oxidative phosphorylation (7), few mitochondria are present in articular chondrocytes (8). Carbohydrate breakdown in articular cartilage is dominated by the conversion of glucose to lactate via the Embden-Meyerhof-Parnas pathway (9–11) that consumes no O_2. Similarly, during the endochondral ossification processes that occur in the growth plate, chondromodulin-1, an endogenous inhibitor of neovascularization, is highly expressed by chondrocytes. Of note, most of the growth plate is avascular (12). Recently, in an *in vivo* experiment, it was found that hypoxia-inducible factor 1, which appears to be one of the major regulators of the hypoxic response, is essential for chondrocyte growth arrest and survival (13). Therefore, hypoxia is considered to be a key factor for the growth and survival of chondrocytes. Chondrocytes are derived from undifferentiated mesenchymal cells that have the potential for multidirectional differentiation (14–16). Bone morphogenetic protein (BMP)[2]-2 promotes the chondrocytic differentiation of undifferentiated mesenchymal cells (17–21). BMP-2 activates Smad1-Smad5-Smad8, which subsequently associates with Smad4, relocates to the nucleus, and regulates the expression of target genes (22, 23). However, the influence of oxygen tension on BMP-Smad signaling remains to be elucidated. In addition to the Smad signaling pathway, p38 mitogen-activated protein kinase (p38 MAPK) is also activated by BMP-2 (24, 25). Several other cytokines (26, 27) or stress signals (28–30) can also activate the p38 MAPK pathway. Of particular interest, hypoxia has been found to be one of the stresses that can phosphorylate and activate p38 MAPK (31). Although p38 MAPK has been shown to be implicated in the regulation of chondrogenesis (32–34), the precise role of p38 MAPK in chondrogenesis remains elusive.

During endochondral ossification, chondrocytes undergo hypertrophy and secrete an extracellular matrix that becomes mineralized and allows vascular invasion and osteoblast differentiation (35, 36). To date, Runx2 and Runx3 (runt-related transcriptional factors 2 and 3) have essential roles in inducing chondrocyte hypertrophy; furthermore, these two interact closely (37–40). In addition, Runx2 is probably a direct tran-

* This work was supported by Ministry of Education, Culture, Sports, Science, and Technology of Japan Grant 15209050. The costs of publication of this article were defrayed in part by the payment of page charges. This article must therefore be hereby marked "*advertisement*" in accordance with 18 U.S.C. Section 1734 solely to indicate this fact.

[1] To whom correspondence should be addressed: Medical Center for Translational Research, Osaka University Hospital, 2-15 Yamadaoka, Suita, Osaka 565-0871, Japan. Tel.: 81-6-6879-6551; Fax: 81-6-6879-6549; E-mail: myoi@hp-mctr.med.osaka-u.ac.jp.

[2] The abbreviations used are: BMP, bone morphogenetic protein; MAPK, mitogen-activated protein kinase; HDAC, histone deacetylase; GAG, glycosaminoglycan; WT-Smad6, wild type Smad6; DN-MKK3, dominant negative form of MKK3; ALP, alkaline phosphatase; TK, thymidine kinase; siRNA, small interfering RNA.

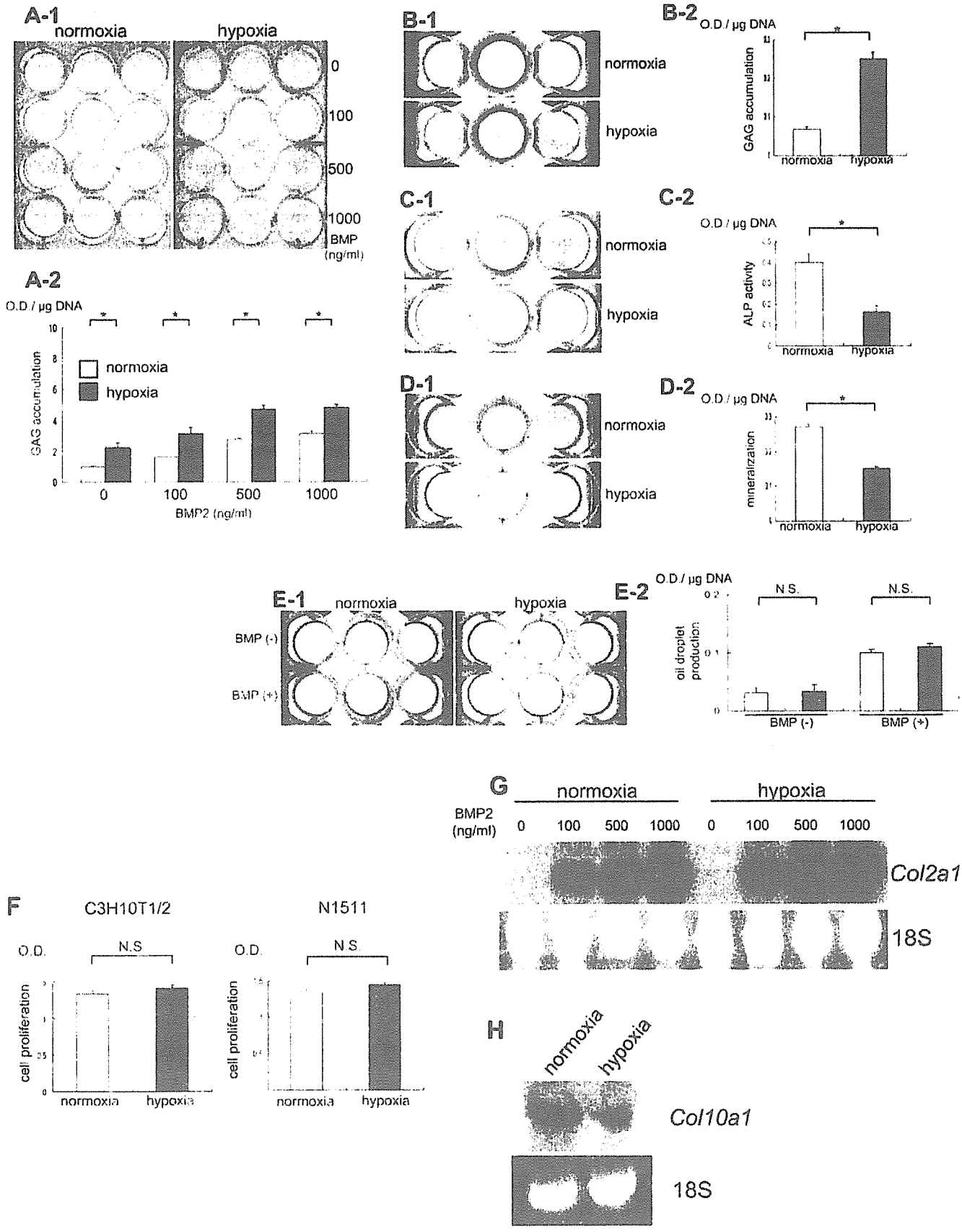

scriptional activator of chondrocyte maturation. It binds *in vivo* to multiple recognition sites in the *Col10a1* promoter and activates *Col10a1* reporter constructs through these elements *in vitro* (41). Runx2 is also necessary for osteoblast differentiation (42, 43). Runx2 transcriptional activity has been shown to be positively regulated both by the Smad pathway and by the p38 MAPK pathway (44–46). HDAC4, a member of the class II histone deacetylases (HDACs), is expressed in prehypertrophic and hypertrophic chondrocytes and regulates chondrocyte hypertrophy and endochondral bone formation by interacting with Runx2. Recently, HDAC4 has been found to inhibit Runx2 expression by repressing its positive feedback mechanism and inhibiting Runx2 activity (47). Although hypoxia has been shown to down-regulate *Runx2* expression in osteoblasts (48), it remains unclear whether Runx2 is involved in the regulation of chondrocyte differentiation and function by oxygen tension.

In the present study, we assessed the influence of oxygen tension on chondrocytic differentiation and cartilage matrix synthesis in the C3H10T1/2 pluripotent mesenchymal cell line and the N1511 murine chondrocyte cell line. We used the mouse embryo organ culture system with wild type mice and Smad6 transgenic mice that we had previously generated. In this paper, we show that hypoxia promotes chondrocytic commitment and cartilage matrix production via the p38 MAPK pathway but that hypoxia inhibits terminal differentiation via the Smad pathway and HDAC4 activation.

EXPERIMENTAL PROCEDURES

Cell Culture and Analysis for Chondrocytic, Osteoblastic, and Adipocytic Differentiation—C3HT101/2 cells were obtained from RIKEN (Saitama, Japan) and were cultured in Dulbecco's modified Eagle's medium (Invitrogen). Since it has been estimated that articular chondrocytes in the deepest layers may have access to no more than 1–6% O_2, we selected 5% O_2 as the hypoxic environment for the cells. The cells were incubated at 37 °C under 5% CO_2 and 20% O_2 (normoxia) or 5% CO_2 and 5% O_2 (hypoxia) with or without recombinant human BMP-2. BMP-2 stimulation was added at 90% confluence. To evaluate chondrocytic differentiation, C3H10T1/2 cells were fixed with 10% formalin, washed with distilled water and 0.1 N HCl, and then stained with Alcian blue solution, Alcian blue 8GX (Sigma). We also cultured N1511 murine chondrocytes (49) and stained with Alcian blue. For the quantitative analysis of chondrocytic differentiation, the absorbance of Alcian blue dyes bound to sulfated glycosaminoglycan (GAG) was measured (50). All experiments were performed in triplicate. To determine osteoblastic differentiation, the C3H10T1/2 cells were fixed with 10% formalin, washed with PBS (pH 7.4) twice, and incubated with alkaline phosphatase (ALP) substrate solution, 0.1 mg/ml naphthol AS-MX (Sigma), and 0.6 mg/ml fast violet B salt (Sigma) in 0.1 M Tris-HCl, pH 8.5. The activity of ALP was also measured using an ALP test kit (Wako, Osaka, Japan) according to the manufacturer's instruction. To evaluate matrix mineralization, the cultures were stained with alizarin red solution (Sigma) (pH 6.0) and incubated in 100 mM cetylpyridinium chloride for 1 h to solubilize and release calcium-bound alizarin red S into solution. The absorbance of the released alizarin red S was measured (51). To determine adipocytic differentiation, the C3H10T1/2 cells were fixed in 10% formalin, washed with diluted water and 60% isopropyl alcohol, and stained with Oil red O (Sigma) solution. Quantitative analysis for oil droplet was performed as described previously (52). To measure the value of absorbance for alcian blue, alizarin red, and oil red O relative to cell density, the absorbance data were normalized by total DNA content. Total DNA content was extracted using a DNeasy tissue kit (Qiagen, Düsseldorf, Germany) and measured. Cell proliferation analysis was also performed. C3H10T1/2 and N1511 cells were cultured in flat bottomed 96-well microplates at a concentration of 1×10^4 cells/ml in Dulbecco's modified Eagle's medium containing 10% fetal bovine serum. After 7 days, cell viability was assessed by cell proliferation assay system kit (Takara Bio Inc., Otsu, Japan), using the sulfonated tetrazolium salt 2-(4-iodophenyl)-3-(4-nitrophenyl)-5-(2,4-disulfophenyl)-2H-tetrazolium monosodium (WST-1).

Organ Culture of Embryonic Limb Explants—The forelimbs from embryonic day 14.5 embryos of ICR wild type mice (Charles River, Osaka, Japan) and Smad6-overexpressing transgenic mice (53) were stripped of skin and muscles. They were then cultured for 5 days in BGJ-B medium (Invitrogen) with 1% penicillin/streptomycin (Invitrogen) and 0.1% fetal bovine serum in organ culture dishes under humidified conditions as previously reported (54–56). Cultures were supplemented with 500 ng/ml BMP-2 under normoxia or hypoxia. After 5 days, limb explants were fixed overnight in 4% paraformaldehyde at 4 °C and embedded in paraffin. Serial 3-μm-thick sections from the wild type mice ($n = 6$) and the transgenic mice ($n = 5$) were processed for safranin O staining and *in situ* hybridization. Briefly, sections were stained with hematoxylin (Sigma) and fast green (Merck) to identify cells and with safranin-O (Sigma) to identify GAGs.

FIGURE 1. **Hypoxia promotes chondrocytic differentiation and GAG production, whereas it suppresses osteoblastic differentiation and chondrocyte terminal differentiation in C3H10T1/2 cell culture.** *A*, C3H10T1/2 cells were cultured with BMP-2 (0, 100, 500, or 1000 ng/ml) under normoxia or hypoxia for 7 days. *A-1*, the cells were stained with alcian blue. *A-2*, BMP-2 induced GAG production in a dose-dependent manner. Data are shown as mean ± S.E. ($n = 3$) OD/μg of DNA. *, $p < 0.01$. *B*, N1511 cells were cultured with 100 ng/ml BMP-2 for 8 days. *B-1*, the cells were stained with alcian blue. *B-2*, quantification of GAG synthesis by N1511 cells. Data were normalized by total DNA content. Data are shown as mean ± S.E. ($n = 3$) OD/μg of DNA. *, $p < 0.001$. *C*, C3H10T1/2 cells were cultured with 500 ng/ml BMP-2 for 7 days. The cells were then stained for ALP activity (*C-1*). *C-2*, quantification of ALP activity. Data are shown as mean ± S.E. ($n = 6$) OD/μg of DNA. *, $p < 0.01$. *D-1*, C3H10T1/2 cells were cultured with 500 ng/ml BMP-2 for 8 days. The cells were then stained with alizarin red solution. *D-2*, quantification of matrix mineralization. Data were normalized by total DNA content. Data are shown as mean ± S.E. ($n = 3$) OD/μg of DNA. *, $p < 0.001$. *E-1*, C3H10T1/2 cells were cultured with or without BMP-2 (500 ng/ml) for 7 days. The cells were stained with oil red O staining solution. *E-2*, quantification of oil droplet production. Data were normalized by total DNA content. Data are shown as mean ± S.E. ($n = 3$) OD/μg of DNA. *N.S.*, not significant. □, normoxia; ■, hypoxia. *F*, cell proliferation analysis was performed 7 days after the culture, as described under "Experimental Procedures." Data are shown as mean ± S.E. ($n = 12$). *, $p < 0.05$; *N.S.*, not significant. *G*, C3H10T1/2 cells were cultured with BMP-2 for 7 days, total RNA was extracted, and Northern blotting analysis was done for *Col2a1* genes (10 μg of total RNA/lane). Expression of 18 S was used to control the amount of RNA. *H*, C3H10T1/2 cells were cultured with 500 ng/ml BMP-2 for 7 days. Total RNA was extracted and subjected to Northern blotting analysis for the *Col10a1* gene.

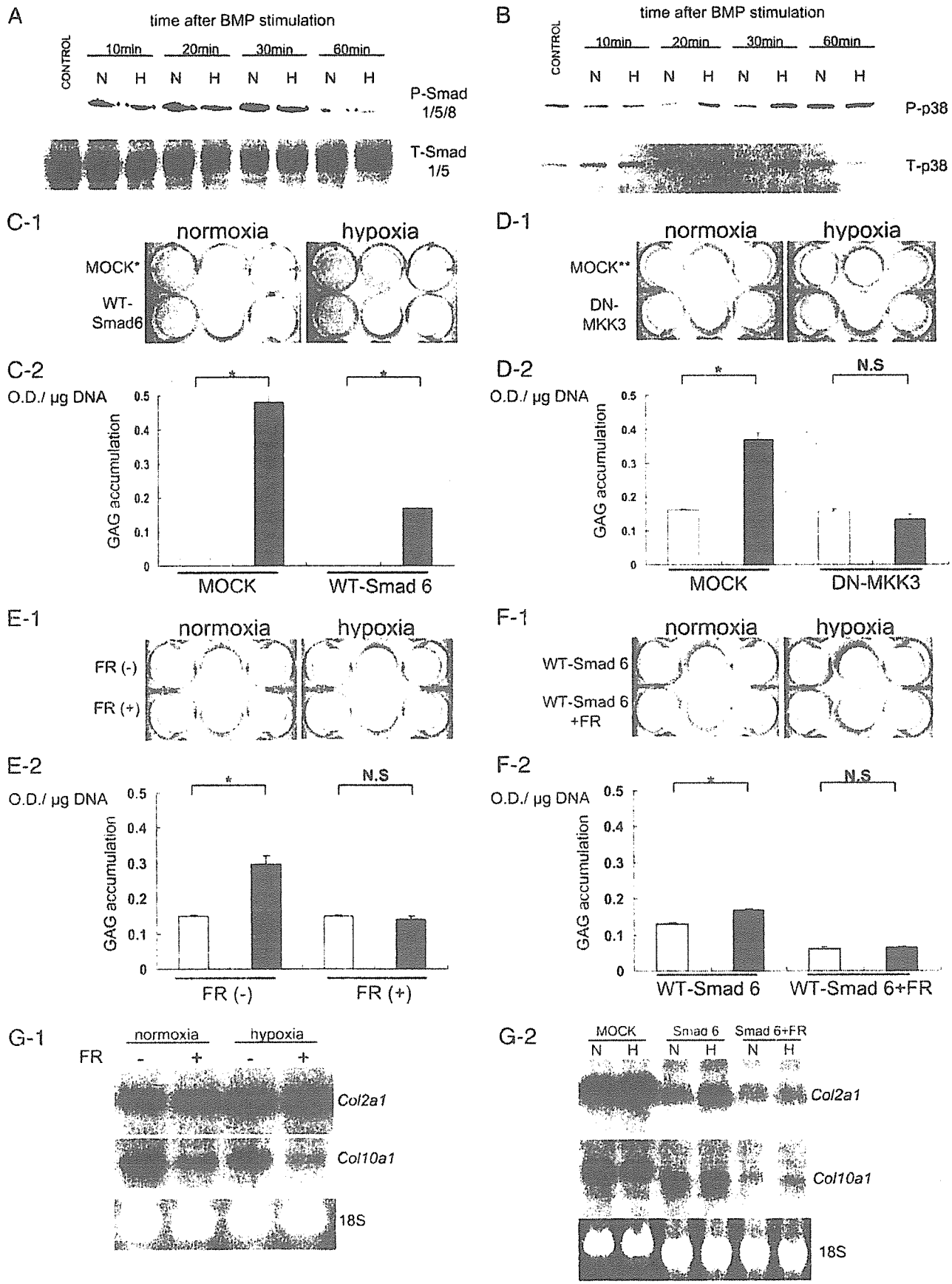

Computer-assisted histological analysis for the proportion of the GAG production area per whole radius was performed using a Nikon ECLIPSE E1000 microscope with a Plan Apo objective, combined with a Nikon DXM 1200 Digital Camera (Tokyo, Japan) and WinRoof image processing software (Mitani Corp.) for Windows. Digitized pictures taken for each radius were analyzed to calculate the ratio of the area stained with safranin-O per whole radius. *In situ* hybridization for *Col10a1* was done as described previously (53, 57). The proportional length of the hypertrophic positive signal of *Col10a1* with respect to the whole hypertrophic chondrocyte zone along the midline was calculated. The care and handling of the animals and the procedures used in this study were in accordance with the guidelines of and were approved by the Osaka University Medical School Animal Care and Use Committee.

Antibodies and Reagents—Anti-phospho-Smad 1/5/8 monoclonal antibody, anti-phospho-p38 MAPK polyclonal antibody, and anti-p38 MAPK monoclonal antibody were purchased from Cell Signaling Technology (Beverly, MA). Anti-Smad 1/5 polyclonal antibody was purchased from Calbiochem. Anti-Sox9 antibody was purchased from Chemicon (Temecula, CA). Anti-HDAC4, anti-β-actin, and antiproliferating cell nuclear antigen polyclonal or monoclonal antibody was purchased from Santa Cruz Biotechnology, Inc. (Santa Cruz, CA). Alexa Fluor® 488 goat anti-rabbit IgG (H + L) antibody was purchased from Molecular Probes, Inc. (Eugene, OR). Hoechst 33342 solution was purchased from Dojindo (Kumamoto, Japan). Recombinant human BMP-2 and a potent p38 MAPK inhibitor, FR167653, were provided by Astellas Pharmaceutical Co., Ltd. (Osaka, Japan).

DNA Constructs—Wild type Smad6 (WT-Smad6)-expressing adenovirus and the dominant negative form of MKK3 (DN-MKK3) vector were donated by Dr. Riko Nishimura (Department of Biochemistry, Osaka University Graduate School, Faculty of Dentistry). Wild type Runx2-expressing vector was donated by Dr. Toshihisa Komori (Department of Developmental and Reconstructive Medicine, Division of Oral Cytology and Cell Biology, Nagasaki University Graduate School of Biomedical Sciences).

Reporter Constructs and Luciferase Reporter Assay—Four tandems of 48-bp chondrocyte-specific enhancer segments of type II collagen α1 (*Col2a1*) were synthesized as previously reported (58) and inserted into the PGL3 promoter vector (Promega), 4Col2E-Luc. Six tandems of the Runx2 binding site were also inserted into the PGL3 promoter vector (Promega), 6Runx2E-Luc. Reporter assays were performed by transient transfection of 0.4 μg of the PGL3-promoter vector (4Col2E-Luc or 6Runx2E-Luc) and 0.01 μg of the TK-*Renilla* luciferase construct (TK *Renilla*) (Promega). Luciferase activity was measured using a Dual Luciferase assay kit (Promega) and luminometer (Berthold Technologies, Bad Wildbad, Germany) and normalized by determining the activity of *Renilla* luciferase. All experiments were performed in triplicate.

RNA Interference—RNA interference was done using commercially synthesized siRNA (Qiagen, Düsseldorf, Germany) and used as described in the protocols provided by the manufacturer. Cells were treated with siRNA to a final concentration of 10 μM. The siRNA duplex sequence targeting the HDAC4 protein was aauguacgacgccaaagautt (sense strands), as previously described (59). Control siRNA consisted of siRNA targeted against luciferase (Dharmacon, Lafayette, CO).

Phosphorylation of Sox9—Serine/threonine phosphorylation of Sox9 was analyzed by affinity chromatography using a phosphoprotein purification kit (Qiagen). Cells were lysed using the lysis buffer provided in the kit. The extracted protein was applied to a phosphorylation purification column, and phosphorylated protein was eluted. Unphosphorylated protein was obtained from the flow-through fraction. These samples were blotted with anti-Sox9 antibody.

Western Blot Analysis—Western blot analyses were performed using whole cell lysates. To detect HDAC4 protein, nuclear extracts were obtained as previously reported (60). The MC3T3-E1 cell (mouse osteoblastic cell) was used as a control. The blots were first incubated with appropriate antibodies and then with horseradish peroxidase-coupled anti-mouse or rabbit IgG antibodies (Amersham Biosciences). For the blots, 20 μg of each sample was applied.

Northern Blot Analysis—Total RNA was isolated from C3H10T1/2 cells using the RNeasy kit (Qiagen). The blots were hybridized with probes for Col2a1, Col10a1, Sox9, and Runx2 mRNA. ^{32}P-Radiolabeled DNA probes were synthesized using cDNA obtained from reverse transcriptase-PCR amplification. The following primers were used: *Col2a1* (forward primer, 5′-CCTGTCTGCTTCTTGTAAAAC-3′; reverse primer, 5′-AAAAAATACAGAGGTGTTTGACACAGA-3′), *Col10a1* (forward primer, 5′-AATCTCATAAATGGGATGGG-3′;

FIGURE 2. **Hypoxia-induced GAG production and *Col2a1* gene expression are mediated by the p38 MAPK pathway rather than the Smad pathway.** *A* and *B*, C3H10T1/2 cells were cultured with or without BMP-2 (500 ng/ml) under normoxia or hypoxia for 10, 20, 30, and 60 min and lysed. The cell lysates were determined by Western blotting with anti-phospho-Smad1-Smad5-Smad8 (*P-Smad 1/5/8*) or anti-Smad1-Smad5 (*T-Smad 1/5*) antibodies (*A*) and with anti-phospho p38 MAPK (*P-p38*) or anti-p38 MAPK (*T-p38*) antibodies (*B*). *N*, normoxia; *H*, hypoxia. *C–F*, regulatory mechanisms of GAG production by hypoxia. □, normoxia; ■, hypoxia. *C*, 12 h after infection with WT-Smad6 adenovirus (*WT-Smad6*), C3H10T1/2 cells were stimulated with BMP-2 (500 ng/ml) and incubated under normoxia or hypoxia. LacZ expression adenovirus (*MOCK**) was used as a control. *C-1*, after 7 days, the cells were stained with alcian blue. *D*, 24 h after transfection with DN-MKK3, C3H10T1/2 cells were stimulated with BMP-2 (500 ng/ml). pGL3 promoter vector (*MOCK***) was used as a control. *D-1*, after 5 days, the cells were stained with alcian blue. *E*, C3H10T1/2 cells were stimulated with BMP-2 (500 ng/ml) in the presence or absence of the p38 MAPK inhibitor, FR167653 (1 μM). The media were changed every 3 days for completely fresh media containing BMP-2 in the presence or absence of FR167653. *FR*, FR167653. *E-1*, after 7 days, the cells were stained with alcian blue. *F*, 12 h after infection with WT-Smad6 adenovirus, C3H10T1/2 cells were stimulated with BMP-2 (500 ng/ml) in the presence or absence of the p38 MAPK inhibitor, FR167653 (1 μM). *F-1*, after 7 days, the cells were stained with alcian blue. *C-2*, *D-2*, *E-2*, and *F-2*, the absorbance of alcian blue dye bound to GAG in each well was quantified (OD/μg of DNA). Data are shown as mean ± S.E. ($n = 3$) (OD/μg of DNA). *, $p < 0.01$; *N.S.*, not significant. *G*, regulatory mechanisms of *Col2a1* and *Col10a1* gene expression by hypoxia. *G-1*, C3H10T1/2 cells were cultured for 5 days with 500 ng/ml BMP-2 in the absence or presence of 1 μM FR167653. Northern blotting analysis for *Col2a1* and *Col10a1* genes was performed (10 μg of total RNA/lane). *G-2*, 12 h after infection with WT-Smad6 adenovirus, the cells were incubated with BMP-2 (500 ng/ml) in the absence or presence of 1 μM FR167653. LacZ expression adenovirus (*MOCK*) was used as a control. Northern blotting analysis for *Col2a1* and *Col10a1* was performed. *N*, normoxia; *H*, hypoxia.

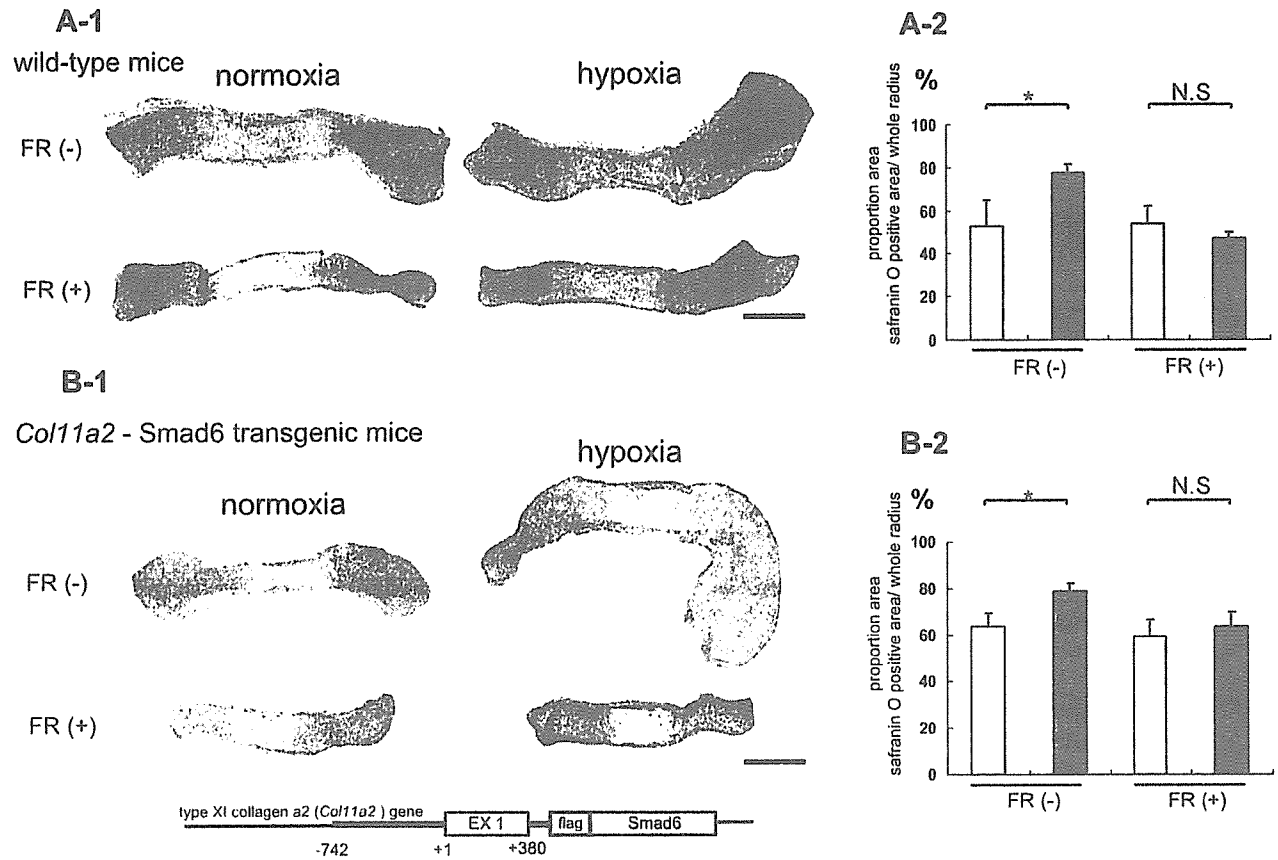

FIGURE 3. **Hypoxia enlarges the cartilaginous matrix area via the p38 MAPK pathway in organ culture system.** *A*, normal mouse embryo forelimb organ culture with BMP-2 (500 ng/ml). *A-1*, histology of the radius of a normal mouse embryo (embryonic day 14.5) visualized with safranin O/fast green/iron hematoxylin staining. *FR(+)*, 1 μM FR167653. *A-2*, morphometric analysis of the forelimb explants. The proportion of the area stained with safranin O per whole radius was measured for each section as described under "Experimental Procedures." Data are shown as mean ± S.E. ($n = 6$). *, $p < 0.05$; *N.S.*, not significant. □, normoxia; ■, hypoxia. *B*, Smad6 transgenic mouse embryo forelimb organ culture. *B-1*, histology of the radius of a Smad6 transgenic mouse embryo (embryonic day 14.5). *B-2*, morphometric analysis of forelimb explants. Data are shown as mean ± S.E. ($n = 5$). *, $p < 0.05$; *N.S.*, not significant. □, normoxia; ■, hypoxia. *Bars*, 240 μm.

reverse primer, 5′-CCTGGGTTAGATGGAAAA-3′), *Sox9* (forward primer, 5′-ATGAATCTCCTGGACCCCTT-3′; reverse primer, 5′-AACTTTGCCAGCTTGCACGT-3′), *Runx2* (forward primer, 5′-GCTTGATGACTCTAAACCTA-3′; reverse primer, 5′-AAAAAGGGCCCAGTTCTGAA-3′). PCR products were purified using the PCR purification kit (Qiagen).

Reverse Transcription PCR Analysis—First-strand cDNA was synthesized using SuperScript II RNase H⁻ reverse transcriptase (Invitrogen). The PCR was performed using Ex Taq (Takara Bio Inc., Otsu, Japan). The primers for the *Runx2* gene were the same as those used for Northern blotting. The GAPDH primers included the forward primer (5′-TGAACGGGAAGCTCACTGG-3′) and the reverse primer (5′-TCCACCACCCTGTTGCTGTA-3′).

Quantitative Real Time PCR Analysis—We obtained cDNA by reverse transcription as mentioned above and proceeded with real time PCR using the Roche Applied Science Light Cycler® system. The SYBR® Green assay, in which each cDNA sample was evaluated in triplicate 20-μl reactions, was used for all target transcripts. Expression values were normalized to GAPDH. The primers for the *Runx2* and GAPDH genes were the same as above. The *Sox9* primers were as follows: forward, 5′-ATGAATCTCCTGGACCCCTT-3′; reverse, 5′-TTGGGGAAGGTGTTCTCCT-3′.

Statistical Analysis—All data are expressed as mean ± S.E. Differences between groups were assessed using Student's *t* test, and differences among three or more groups were assessed by *post hoc* testing. A *p* value of <0.05 was considered statistically significant.

RESULTS

Hypoxia Promotes Chondrocytic Differentiation and GAG Production, whereas It Suppresses Osteoblastic Differentiation and Chondrocyte Terminal Differentiation in C3H10T1/2 Cell Culture—In C3H10T1/2 cell culture, BMP-2 induced GAG production in a dose-dependent manner (Fig. 1*A*). At every BMP-2 concentration tested, hypoxia clearly increased GAG content additively with BMP-2. Hypoxia-induced GAG synthesis was also found in the N1511 murine chondrocyte culture (Fig. 1*B*). On the other hand, low oxygen tension clearly suppressed ALP activity and alizarin red staining of C3H10T1/2 cells (Fig. 1, *C* and *D*), suggesting that hypoxia suppressed BMP-2-induced osteoblastic differentiation. Adipocytic differentiation, as identified by oil red O staining, was not affected by

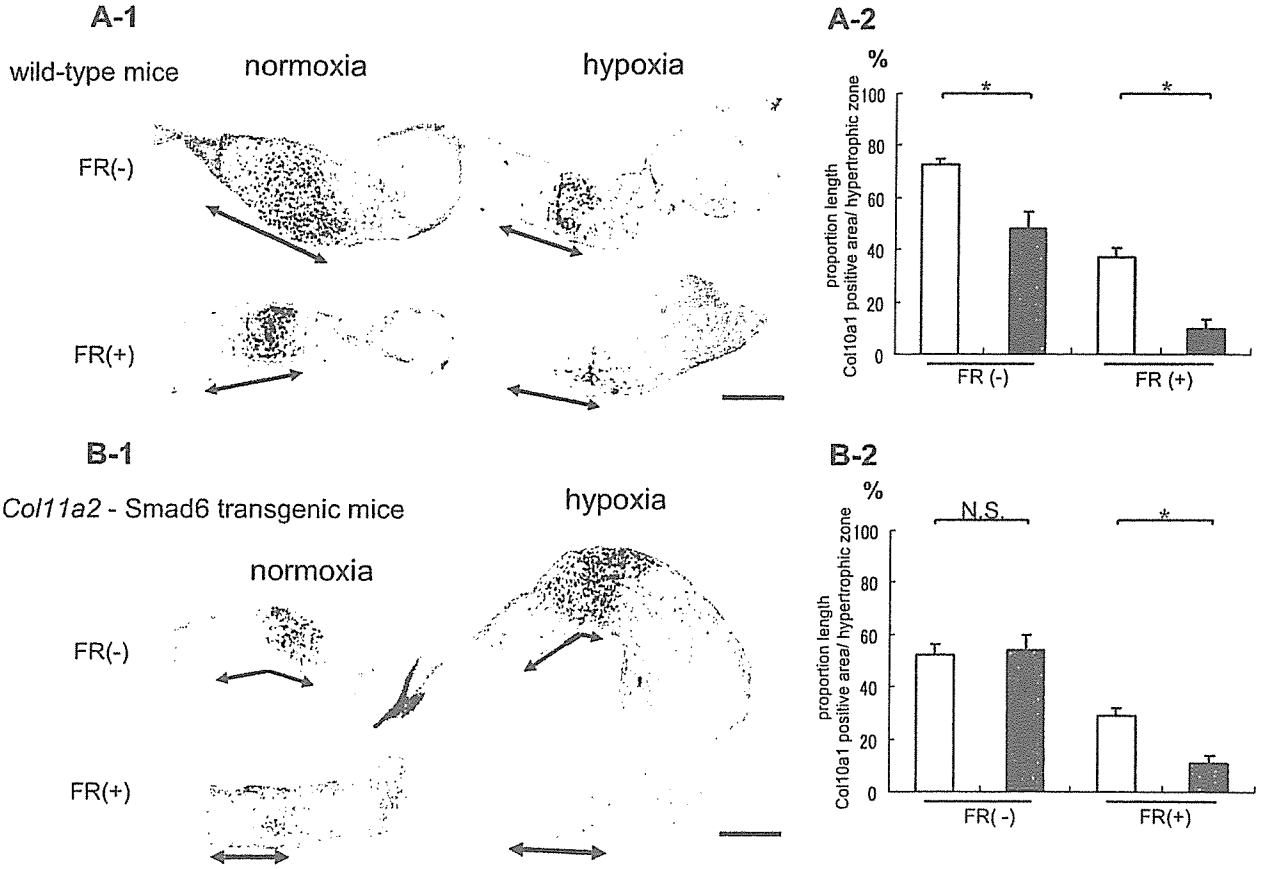

FIGURE 4. **Terminal differentiation of chondrocytes is suppressed by hypoxia in mouse embryo organ cultures.** *A*, normal mouse embryo forelimb organ culture. *A-1*, sections of normal mice forelimbs were hybridized with cRNA probes for *Col10a1*. *FR(+)*, 1 μM FR167653. *A-2*, the proportion of the length of *Col10a1* mRNA expression site per hypertrophic chondrocyte zone (*bidirectional arrow*) along the midline was measured for each section. Data are shown as mean ± S.E. ($n = 6$). *, $p < 0.05$; **, $p < 0.01$; □, normoxia; ■, hypoxia. *B*, Smad6 transgenic mouse embryo forelimb organ culture. *B-1*, sections of Smad6 transgenic mouse forearms were hybridized with cRNA probes for *Col10a1*. *B-2*, morphometric analysis of the forelimb explants. Data are shown as mean ± S.E. ($n = 5$). *, $p < 0.05$; *N.S.*, not significant. □, normoxia; ■, hypoxia. *Bars*, 120 μm.

oxygen tension (Fig. 1*E*). After cell density became confluent, there was no difference of the cell proliferation between normoxia and hypoxia at 7 days in C3H10T1/2 cells and N1511 cells (Fig. 1*F*). The type II collagen α1 (*Col2a1*) gene, a well characterized, specific marker of commitment to the chondrogenic lineage, was up-regulated by BMP-2 in a dose-dependent manner (Fig. 1*G*) as well as by hypoxia at each BMP-2 concentration tested. The mRNA expression of the type X collagen α1 (*Col10a1*) gene, a well characterized, specific marker for chondrocyte terminal differentiation (61, 62), was suppressed by hypoxia (Fig. 1*H*), in contrast to *Col2a1* mRNA expression.

Hypoxia-induced GAG Production Is Mediated by the p38 MAPK Pathway rather than the Smad Pathway—To investigate the intracellular signal transduction mechanisms responsible for hypoxia-induced chondrocyte differentiation, we first examined the activities of the Smad and the p38 MAPK pathways. As shown in Fig. 2, *A* and *B*, phosphorylation of p38 MAPK is up-regulated by hypoxia, whereas phosphorylation of Smad is down-regulated. When Smad signaling was inhibited by the overexpression of WT-Smad6, which inhibits phosphorylation of the Smad1-Smad5-Smad8 complex, BMP-2-induced GAG production was markedly reduced under both oxygen levels. However, hypoxia was still able to promote GAG production despite Smad inhibition (Fig. 2*C*). In contrast, hypoxia-induced GAG production was abolished by the overexpression of DN-MKK3 that specifically inhibits p38 MAPK phosphorylation (Fig. 2*D*) and also by FR167653, a specific p38 MAPK inhibitor (Fig. 2*E*). When both the Smad and the p38 MAPK pathways were blocked by Smad6 overexpression and FR167653, hypoxia did not influence the GAG production level (Fig. 2*F*).

Regulatory Mechanisms of Col2a1 and Col10a1 Gene Expression by Oxygen Tension—Next, we assessed the role of the p38 MAPK and Smad pathways in the regulation of *Col2a1* and *Col10a1* gene expression. In the presence of FR167653, hypoxia-induced *Col2a1* expression was suppressed (Fig. 2, *G-1*). However, when WT-Smad6 was overexpressed, although *Col2a1* gene expression was suppressed under both oxygen conditions, hypoxia strongly induced the *Col2a1* gene. When both Smad and p38 MAPK signaling was blocked by WT-Smad6 and FR167653, *Col2a1* gene induction caused by hypoxia was again strongly attenuated (Fig. 2, *G-2*). Our findings suggest that hypoxic regulation of *Col2a1* gene expression is mediated by the p38 MAPK pathway rather than the Smad pathway, which is very similar to the mechanism of hypoxic regulation involved in GAG production. On the other hand,

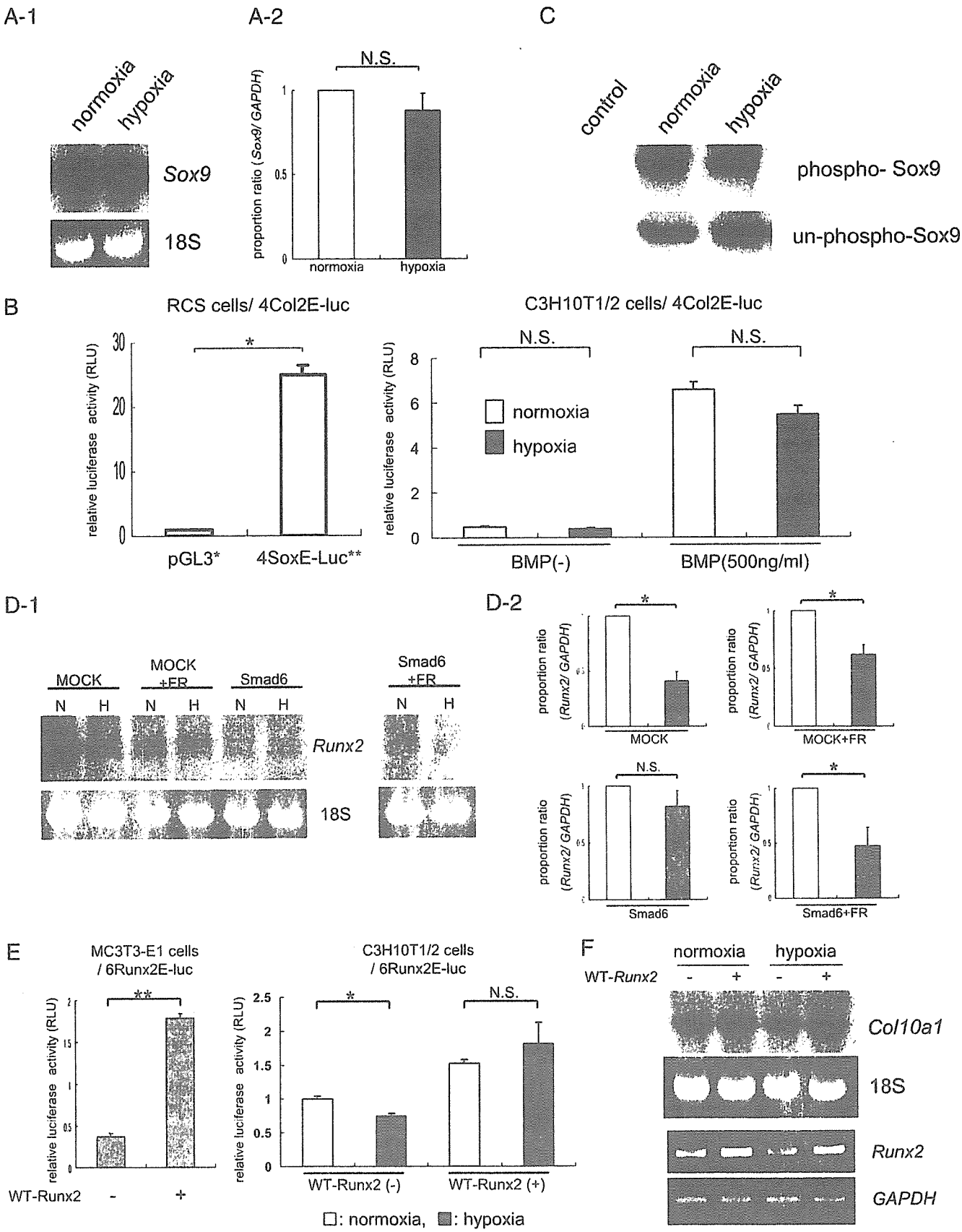

Col10a1 gene expression was reduced by hypoxia as shown in Fig. 1*G*, and it seemed to be regulated in a complicated manner that is different from *Col2a1* gene expression. The blockade of the p38 MAPK pathway did not alter the hypoxia-related reduction of *Col10a1* gene expression, but the blockade of the Smad pathway abolished it. However, when both pathways were blocked, hypoxia reduced *Col10a1* gene expression (Fig. 2*G*).

Hypoxia Enlarges the Cartilaginous Matrix Area Associated with Endochondral Ossification via the p38 MAPK Pathway in Organ Culture—Our data show that hypoxia promoted the commitment of C3H10T1/2 cells to a chondrocytic lineage and enhanced cartilage matrix production via the p38 MAPK pathway. To further confirm the influence of oxygen tension on cartilage biology in a setting similar to that found *in vivo*, we cultured embryonic day 14.5 embryo forelimbs obtained from wild type and Smad6 transgenic mice. In *ex vivo* embryo limb cultures in the presence of BMP-2, explants grew quickly both in length and in width and wound greatly as they grow. Therefore, to evaluate cartilaginous matrix production, we calculated the proportion of the area of each radius that was stained with safranin-O compared with the whole radius area. The embryo forelimbs that were cultured under hypoxic conditions showed a significantly greater enlargement in the matrix area, and hypoxia-induced cartilage enlargement was abolished by FR167653 (Fig. 3, *A-1*). In explants from Smad6 transgenic mice, hypoxia enlarged the cartilage matrix area, and FR167653 abolished hypoxia-induced matrix enlargement (Fig. 3, *B-1*). These findings are consistent with our *in vitro* observation that hypoxia promotes cartilaginous matrix synthesis not via the Smad pathway but via p38 MAPK signaling (Fig. 2*G*).

Terminal Differentiation of Chondrocyte Is Suppressed by Hypoxia in Mouse Embryo Organ Cultures—In C3H10T1/2 cell cultures, *Col10a1* gene expression was repressed by hypoxia. In accordance with this, when using *in situ* hybridization, we found that, in wild type embryo forelimb cultures, hypoxia reduced the *Col10a1* gene expression level estimated by the proportional length of the *Col10a1*-positive site per whole hypertrophic chondrocyte zone (Fig. 4, *bidirectional arrows*) along the midline. When p38 MAPK signaling was suppressed using FR167653, the *Col10a1*-positive area was markedly reduced with both oxygen levels. In addition, hypoxia apparently reduced the *Col10a1*-positive area regardless of the use of p38 MAPK inhibitor (Fig. 4*A*). On the other hand, hypoxia alone did not repress *Col10a1* gene expression in Smad6 transgenic mice embryo forelimb organ culture, although hypoxia did suppress *Col10a1* gene expression when the p38 MAPK pathway was inhibited by FR167653 (Fig. 4*B*). These findings were in agreement with the *in vitro* results and suggest that the Smad pathway mediates *Col10a1* gene down-regulation and that the p38 MAPK pathway mediates its up-regulation. In addition, hypoxia reduced *Col10a1* expression even when both Smad and p38 MAPK signaling were blocked, which would suggest that unknown factors that down-regulate *Col10a1* gene expression are involved.

Sox9 Gene Expression and Its Transcriptional Activity Are Not Up-regulated by Hypoxia—Sox9 is a key transcriptional factor for chondrocytic differentiation and regulates transcription of the *Col2a1* gene. Thus, we evaluated the influence of oxygen tension on *Sox9* gene expression. Interestingly, *Sox9* mRNA expression was not altered by hypoxia (Fig. 5*A*). As shown in Fig. 5*B*, Sox9 transcriptional activity was clearly up-regulated by BMP-2. However, it was not up-regulated but rather was down-regulated by hypoxia. *Sox9* transcriptional activity has been reported to be enhanced by cAMP-dependent protein kinase A serine/threonine phosphorylation (63). We found that phosphorylation of Sox9 was not promoted but was suppressed by hypoxia (Fig. 5*C*), which was consistent with the results of the reporter assay.

Runx2 Gene Expression and Its Transcriptional Activity Are Suppressed by Hypoxia—Since hypoxia suppressed chondrocyte hypertrophy and osteoblastic differentiation, we studied the role of Runx2 in the regulation of hypoxia-induced phenomena. Hypoxia suppressed *Runx2* gene expression and its transcriptional activity in C3H10T1/2 cells stimulated with BMP-2 (Fig. 5, *D* and *E*). Blockade of the p38 MAPK pathway did not alter the suppression of *Runx2* caused by hypoxia, but blockade of the Smad pathway abolished the effect of hypoxia. However, when both pathways were blocked, hypoxia could again suppress *Runx2* gene expression (Fig. 5*D*). This pattern is very similar to the regulatory pattern we found for the hypoxic regulation of *Col10a1* gene expression. To examine how Runx2 contributes to chondrocyte terminal differentiation in hypoxia, we transfected C3H10T1/2 cells with vector expressing wild type Runx2. When Runx2 was overexpressed, the Runx2 transcriptional activity suppressed by hypoxia was remarkably up-regulated to a level comparable with that with normoxia (Fig. 5*E*). In addition, *Col10a1* gene expression that had been reduced by hypoxia recovered to a level that matched the level expressed under normoxic conditions with Runx2 overexpres-

FIGURE 5. **Gene expression and transcriptional activity of Sox9 (*A–C*) and Runx2 (*D–F*) under hypoxia.** *A-1*, C3H10T1/2 cells were stimulated with BMP-2 (500 ng/ml) for 5 days. Total RNA was extracted, and Northern blotting was done for *Sox9*. *A-2*, real time PCR for the *Sox9* gene was performed. Data are shown as mean ± S.E. ($n = 3$) of the proportion ratio for *Sox9* gene expression as compared with normoxia. *N.S.*, not significant. *B*, C3H10T1/2 cells were co-transfected with 4Col2E-Luc and TK-*Renilla* reporter constructs. As a control, the rat chondrosarcoma cell line (*RCS*) was used. 12 h after transfection, cells were incubated with or without BMP-2 (500 ng/ml) for 5 days. Luciferase activity was measured and normalized by determining *Renilla* luciferase activity. Data are shown as mean ± S.E. ($n = 3$). *, $p < 0.0001$; *N.S.*, not significant. *C*, C3H10T1/2 cells were cultured for 5 days and lysed. The cell lysate was immunoprecipitated with anti-phosphoserine and phosphothreonine antibodies and blotted with anti-*Sox9* antibodies. *D-1*, 12 h after infection with WT-Smad6 adenovirus, the cells were stimulated with BMP-2 (500 ng/ml) in the absence or presence of 1 μM FR167653. As a control, LacZ expression adenovirus (*MOCK*) was used. After 48 h, total RNA was extracted, and Northern blotting for the *Runx2* gene was performed. *N*, normoxia; *H*, hypoxia. *D-2*, real time PCR for *Runx2* gene was performed. Data are shown as mean ± S.E. ($n = 3$) of the proportion ratio for *Runx2* gene expression as compared with normoxia. *, $p < 0.001$; *N.S.*, not significant. □, normoxia; ■, hypoxia. *E*, C3H10T1/2 cells were co-transfected with 6Runx2E-Luc and TK-*Renilla* reporter constructs. As a control, the mouse osteoblast cell line (MC3T3-E1) was used. 24 h after transfection, cells were incubated with BMP-2 (500 ng/ml) for 2 days, and relative luciferase activity was measured and normalized by determining *Renilla* luciferase activity. Data are shown as mean ± S.E. ($n = 3$). *, $p < 0.05$; **, $p < 0.0002$; *N.S.*, not significant. *F*, 24 h after transfection with wild type Runx2, the cells were stimulated with BMP-2 (500 ng/ml) and incubated under normoxia or hypoxia for 5 days. As a control, the cells were transfected with pGL3 promoter vector. Then Northern blotting for *Col10a1* genes was performed.

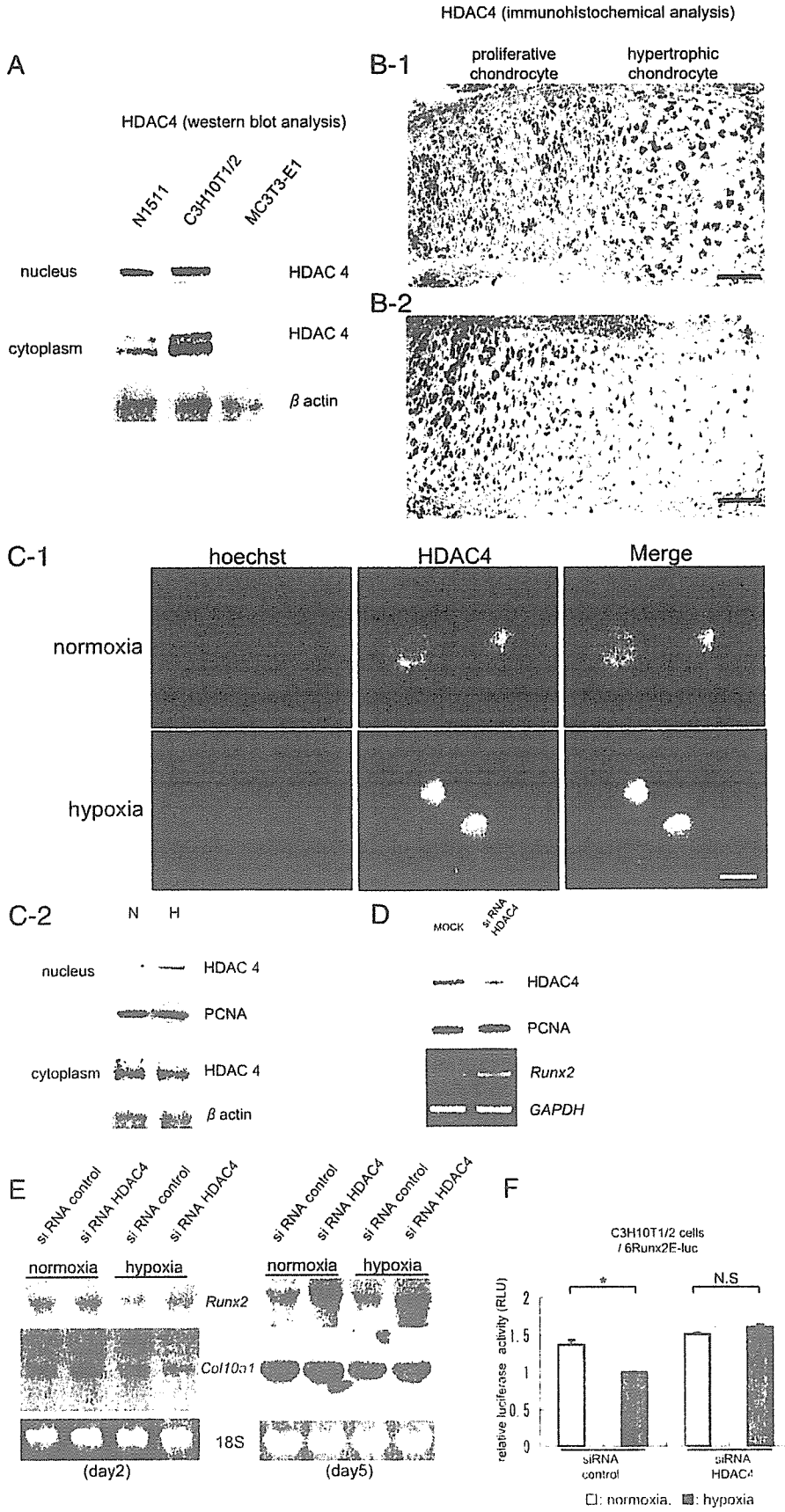

sion (Fig. 5*F*). These data suggest that Runx2 mediates *Col10a1* gene suppression by hypoxia and that a third regulatory mechanism, independent of the Smad and the p38 MAPK pathways, is involved in the regulation by oxygen tension of *Runx2* gene expression.

HDAC4 Is Expressed by Chondrocytes and Accumulates in the Nucleus under Hypoxia—Recently, it was reported that HDAC4 inhibits chondrocyte hypertrophy by suppressing *Runx2* gene expression. HDAC4 has been reported to be expressed by chondrocytes in the prehypertrophic and hypertrophic zones (47). We could detect HDAC4 only in chondrocytic lineage cells (N1511 or C3H10T1/2) and almost not in osteoblastic cells (MC3T3-E1) (Fig. 6*A*). We furthermore confirmed that HDAC4 protein was expressed in the hypertrophic chondrocytes of the growth plate but not in proliferative chondrocytes (Fig. 6*B*). To elucidate whether HDAC4-Runx2 regulation is involved in the hypoxic suppression of terminal differentiation, we first examined the effect of oxygen tension on HDAC4 activation. Our immunofluorescence study revealed that the expression pattern of HDAC4 changed from being located in the cytoplasm to being located in the nucleus when cells were incubated under hypoxic conditions (Fig. 6, *C-1*). Accordingly, HDAC4 protein expression in the nuclear extract by Western blotting was up-regulated after 24 h of hypoxic stimulation (Fig. 6, *C-2*).

Inhibition of HDAC4 Up-regulates Runx2 Gene Expression and Its Transcriptional Activity and Restores Col10a1 Gene Expression That Is Decreased by Hypoxia—To evaluate whether HDAC4 is involved in the hypoxic regulation of *Runx2* and *Col10a1* gene expression, we inhibited HDAC4 by RNA interference (Fig. 6*D*). The inhibition of HDAC4 partly restored the reduced *Runx2* gene expression that resulted from 2 days of hypoxia. On day 5, *Runx2* gene expression was clearly promoted by HDAC4 silencing regardless of oxygen level, and the hypoxia-induced suppression of *Runx2* expression was completely restored to that seen with normoxia (Fig. 6*E*). Consistent with these results, HDAC4 inhibition completely abolished the reduction of Runx2 transcriptional activity caused by hypoxia (Fig. 6*F*). As a consequence, after 5 days of hypoxic stimulation, *Col10a1* gene expression that had been suppressed by hypoxia was also up-regulated by HDAC4 inhibition and recovered to the level seen with normoxia. These data strongly suggested that hypoxia activates HDAC4, which in turn suppresses Runx2 activity and subsequently leads to the reduction of *Col10a1* gene expression.

DISCUSSION

Murine mesenchymal C3H10T1/2 cells are pluripotent and differentiate into several lineages (19). BMP-2 and BMP-7 induce C3H10T1/2 cells to differentiate into osteoblasts, chondrocytes, and adipocytes; a low concentration favors adipocytes, and a high concentration favors chondrocytes and osteoblasts (18, 19, 64, 65). Thus, C3H10T1/2 cells are an appropriate model for studying the mechanisms of pluripotent mesenchymal cell commitment into a particular lineage. In the present study, we cultivated C3H10T1/2 cells in the presence or absence of recombinant human BMP-2 under normoxia or hypoxia. BMP-2 treatment and low oxygen tension synergistically induced GAG production and *Col2a1* gene expression and profoundly suppressed ALP activity and mineralization; they did not alter fat droplet production. These data indicate that hypoxia promoted chondrocytic commitment of the pluripotent C3H10T1/2 mesenchymal cells and inhibited osteoblastic differentiation. Our results are in accordance with previous reports, which describe that hypoxia enhances *Col2a1* and Aggrecan gene expression in C3H10T1/2 cells (66). To further investigate the role of oxygen tension in chondrocytic differentiation, we used a mouse embryo forelimb explant culture system. This system enables one to cultivate cartilage tissue under hypoxic conditions for up to 2 weeks without any interference from systemic, hormonal, or neuronal responses to the hypoxia that could affect cartilage metabolism while at the same time examining the effects of both environmental factors and cytokines on the endochondral ossification process. In organ cultures of wild type mice forelimbs at 14.5 days postcoitum, we found that hypoxia clearly induced the enlargement of the cartilage matrix area stained by Safranin-O, suggesting that hypoxia promoted cartilage matrix synthesis by chondrocytes during endochondral ossification. To confirm this, we cultured N1511 chondrocytes under hypoxic conditions and found that hypoxia induced N1511 cells to produce GAG. Our data indicate that hypoxia not only induced the commitment of pluripotent mesenchymal progenitors into a chondrocyte lineage but also activated the production by chondrocytes of cartilage matrix.

In the present study, hypoxia in the presence of BMP-2 clearly suppressed *Col10a1* mRNA expression in C3H10T1/2 cell culture and also in organ culture studies using tissues from wild type animals. This suggests that hypoxia suppresses the terminal differentiation of chondrocytes during endochondral

FIGURE 6. **With hypoxia, HDAC4 accumulates in the nucleus and down-regulates Runx2 expression, Runx2 transcriptional activity, and *Col10a1* gene expression.** *A*, nuclear and cytoplasmic extracts from C3H10T1/2, N1511, and MC3T3-E1 cells (mouse osteoblastic cells) were examined by Western blotting with anti-HDAC4 antibodies. Mixed lysate (nuclear extract (10 μg) plus cytoplasmic extracts (10 μg)) was blotted for β-actin for the control. *B*, immunohistochemical analysis for HDAC4 protein in normal mouse embryo humerus (embryonic day 14.5). *Bars*, 30 μm. *B-1*, HDAC4 protein expression in hypertrophic chondrocytes, not in proliferative chondrocytes. *B-2*, negative control without primary antibody. *C*, nuclear translocation of HDAC4 protein by hypoxia. *C-1*, immunofluorescence staining for HDAC4 protein. After starvation for 24 h, C3H10T1/2 cells were stimulated with BMP-2 (500 ng/ml) and further incubated under normoxia or hypoxia for 1 h. Immunofluorescence staining was performed using anti-HDAC4 antibody (1:100) for 2 h followed by Alexa Fluor 488 for 30 min. Hoechst 33342 was used for nucleus staining. *Bar*, 12.5 μm. *C-2*, nuclear and cytoplasmic extracts from C3H10T1/2 cells were harvested and examined by Western blotting with anti-HDAC4 antibodies. Proliferating cell nuclear antigen and β-actin acted as the internal loading control for nuclear and cytoplasmic fractions, respectively. *N*, normoxia; *H*, hypoxia. *D*, 24 h after transfection with siRNA for HDAC4, nuclear extracts from the cells were harvested and analyzed by Western blotting with anti-HDAC4 antibodies. Proliferating cell nuclear antigen acted as the internal loading control for nuclear fractions. After transfection with siRNA for HDAC4, the cells were incubated for 5 days, and reverse transcription-PCR analysis for *Runx2* was done. *E*, 24 h after transfection with siRNA for HDAC4, the cells were stimulated by 500 ng/ml BMP-2 for either 48 h or 5 days. Northern blotting for *Runx2* and *Col10a1* were done. *F*, C3H10T1/2 cells were co-transfected with siRNA, 6Runx2E-Luc, and TK-*Renilla* reporter constructs. 24 h after transfection, cells were incubated with BMP-2 (500 ng/ml) for 48 h under normoxia or hypoxia. At the end of the culture, relative luciferase activity was determined. Data are shown as mean ± S.E. (n = 3). *, $p < 0.05$; *N.S.*, not significant.

ossification. Thus, hypoxia seems to act on chondrocytes to preserve their chondrocyte phenotype by preventing hypertrophy and, consequently, terminal differentiation.

To confirm the mechanisms by which these hypoxia-induced phenomena operate, we studied the signaling pathways of BMP-2 that are well known to induce chondrogenesis of mesenchymal cells (17–21) via the induction of *Sox9* gene expression (67). Basically, BMP-2 signals propagate through the Smad pathway and bind directly or via other DNA-binding proteins to the promoters of BMP-2-responsive genes to stimulate or repress their transcription. Over the past few years, evidence has accumulated that suggests that BMP-2 may also stimulate other downstream pathways involving p38 MAPK. In the present study, we found that hypoxia enhanced BMP-2-induced activation of the p38 MAPK pathway, whereas hypoxia did not promote and could even suppress the Smad pathway. Furthermore, our Smad- and p38 MAPK-suppressing studies using WT-Smad6, DN-MKK3, and FR167653 revealed that it is not the Smad pathway but the p38 MAPK pathway that is indispensable for hypoxia-induced cartilaginous matrix synthesis. Overall, our data indicate that hypoxia promotes cartilaginous matrix synthesis via the p38 MAPK pathway.

Little is known about how oxygen tension regulates the signal transduction systems that regulate *Col10a1* gene expression. In the present study, we found that hypoxia promoted BMP-2-induced activation of the p38 MAPK pathway but did not promote, and could even suppress, the Smad pathway. Previous reports suggested that Smad1-Smad5 signaling positively regulates type X collagen expression by potentiating the transcriptional activity of Runx2 (44, 45) and that p38 MAPK signaling also promotes its expression (34, 45, 68) via Runx2 activation. These observations are consistent with the results of our experiments that blocked these pathways by Smad6, DN-MKK3, or the p38 inhibitor, FR167653. This suggests that hypoxia positively regulates *Col10a1* gene expression via the up-regulation of p38 MAPK signaling and negatively regulates *Col10a1* gene expression via down-regulation of the Smad pathway. In addition to this, we found that hypoxia up-regulated HDAC4 activity, which recently was reported to control chondrocyte hypertrophy by suppressing *Runx2* gene expression through inhibition of the gene's positive feedback mechanism and the suppression of its transcriptional activity (47). We were able to confirm that hypoxic suppression of *Runx2* gene expression, transcriptional activity, and *Col10a1* gene expression were blocked by silencing HDAC4. This indicates that hypoxia activates HDAC4, thereby suppressing Runx2 activity, which in turn down-regulates *Col10a1* gene expression. Our data reveal that hypoxia inhibits the hypertrophy of chondrocytes by down-regulating Runx2 activity based on the sum of the positive regulation that occurs via p38 MAPK activation and the negative regulation that is caused by Smad signaling suppression and HDAC4 activation.

Transcriptional factors Sox9, L-Sox5, and Sox6, have been reported to be essential and sufficient for regulating the expression of *Col2a1* and the other genes involved in the chondrocytic program (69). This would suggest that Sox transcriptional factors should be up-regulated by hypoxia and thus propagate the signals for chondrocytic differentiation and cartilage matrix

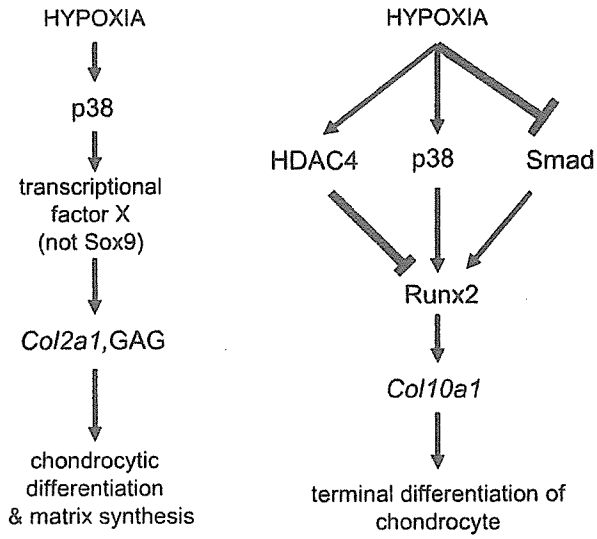

FIGURE 7. **Proposed models of the regulatory mechanisms responsible for chondrocyte differentiation and function based on oxygen level.** Hypoxia enhances the p38 MAPK pathway and suppresses the Smad pathway. Activated p38 MAPK signaling promotes *Col2a1* gene expression and GAG production independently of the Smad pathway and *Sox9*. Hypoxia inhibits *Col10a1* gene expression by reducing Runx2 activity based on the sum of the positive regulation via p38 MAPK activation and the negative regulation caused by Smad signaling suppression and HDAC4 activation.

production. However, very interestingly, our results indicate that hypoxia-mediated chondrocytic differentiation did not involve the up-regulation of *Sox9* gene expression, its phosphorylation, or its transcriptional activity, suggesting that hypoxia-induced *Col2a1* induction was independent of Sox9. However, in the previous report, it was described that *Sox9* gene expression was up-regulated by hypoxia in association with transactivation of the *Sox9* promoter in ST2 stromal cells (66). Although the difference in the results might depend on the difference in cell type, further confirmation about the *Sox9* promoter may be necessary. The results of the reporter assay lead us to speculate that transcription factors other than Sox9 directly regulate *Col2a1* gene expression via other cis elements located at a site other than the chondrocyte-specific enhancer fragment of the *Col2a1* gene (69, 70). The Sox trio shares a cis element in the *Col2a1* chondrocyte-specific enhancer region; however, to exclude the involvement of L-Sox5 and Sox6 in hypoxia-induced *Col2a1* gene expression, further confirmation, including gene expression of these transcription factors, is needed. It is known that hypoxic stress reduces protein kinase A activity (71). Recently, protein kinase A was reported to phosphorylate Sox9 and to enhance its transcriptional activity (62). Taking these data into account, it is plausible that Sox9 transcriptional activity could have been down-regulated by hypoxia. However, the actual transcription factors responsible for hypoxia-induced *Col2a1* induction remain to be elucidated (Fig. 7).

In conclusion, we demonstrated that hypoxia clearly promoted chondrocytic commitment of cells in the mesenchymal lineage, as well as cartilaginous matrix synthesis, and inhibited terminal differentiation both in cell culture and organ culture. These effects were primarily mediated by p38 MAPK activation

independent of Sox9. On the other hand, hypoxia inhibited the hypertrophy of chondrocytes via the down-regulation of Runx2 activity through Smad signaling suppression and HDAC4 activation. These hypoxia-induced phenomena affect mesenchymal cell differentiation and endochondral ossification by enhancing and preserving the chondrocytic phenotype and cell function, as well as preventing chondrocytes from terminal differentiation that subsequently leads to matrix degeneration and chondrocyte apoptosis. The hypoxia-associated regulation of chondrocytes that has been outlined in our study may be of fundamental importance in the biology and pathology of cartilage tissues and may be involved in endochondral ossification in the growth plate, in joint cartilage homeostasis, and in the etiology of osteoarthritis.

Acknowledgments—We thank Dr. Riko Nishimura for valuable comments on this work and for donating the dominant negative MKK3 vector and the wild type Smad6 expression adenovirus; Dr. Toshihisa Komori for donating the wild type Runx2 expression vector; and Dr. Hideto Watanabe and Dr. Nobuhiro Kamiya for donating the N1511 cells. We also thank Kaori Sudo for excellent technical assistance and Astellas Pharmaceutical. Co. Ltd. for supplying recombinant human BMP-2 and FR167653.

REFERENCES

1. Falchuk, K. H., Goetzl, E. J., and Kulka J. P. (1970) *Am. J. Med.* **49,** 223–231
2. Olesen, L. L. (1970) *Arthritis Rheum.* **13,** 769–776
3. Treuhaft, P. S., and McCarthy, D. J. (1971) *Arthritis Rheum.* **14,** 475–484
4. Silver, I. A. (1975) *Philos. Trans. R. Soc. Lond. B Biol. Sci.* **271,** 261–272
5. Kiaer, T., Gronlund, J., and Sorensen, K. H. (1988) *Clin. Orthop. Relat. Res.* **229,** 149–155
6. Ferrell, W. R., and Najafipour, H. (1992) *J. Physiol.* **449,** 607–617
7. Lee, N. H., and Shapiro, I. M. (1974) *Calcif. Tissue Res.* **16,** 277–282
8. Brighton, C. T., Kitajima, T., and Hunt, R. M. (1984) *Arthritis Rheum.* **27,** 1290–1299
9. Marteus, R. E. (1973) *Arthritis Rheum.* **16,** 646–656
10. Otte, P. (1991) *Z. Rheumatol.* **50,** 304–312
11. Lee, R. B., and Urban, J. P. G. (1997) *Biochem. J.* **321,** 95–102
12. Hiraki, Y., Inoue, H., Iyama, K., Kamizono, A., Ochiai, M., Shukunami, C., Iijima, S., Suzuki, F., and Kondo, J. (1997) *J. Biol. Chem.* **272,** 32419–32426
13. Scipani, E., Ryan, H. E., Didrickson, S., Kobayashi, T., Knight, M., and Johnson, R. S. (2001) *Genes Dev.* **15,** 2865–2876
14. Johnstone, B., Hering, T. M., Caplan, A. I., Goldberg, V. M., and Yoo, J. U. (1998) *Exp. Cell Res.* **238,** 265–272
15. Huang, C. Y., Reuben, P. M., Ippolito, G. D., Schiller, P. C., and Cheung, H. S. (2004) *Anat. Rec.* **278,** 428–436
16. Bosnakovski, D., Mizuno, M., Kim, G., Ishiguro, T., Okumura, M., Iwanaga, T., Kadosawa, T., and Fujinaga, T. (2004) *Exp. Hematol.* **32,** 502–509
17. Shukunami, C., Ohta, Y., Sakuda, M., and Hiraki, Y. (1998) *Exp. Cell Res.* **241,** 1–11
18. Asahina, I., Sampath, T. K., and Hauschka, P. V. (1996) *Exp. Cell Res.* **222,** 38–47
19. Wang, E. A., Israel, D. I., Kelly, S., and Luxenburg, D. P. (1993) *Growth Factors* **9,** 57–71
20. Atkinson, B. L., Fantle, K. S., Benedict, J. J., Huffer, W. E., and Gutierres-Hartmann, A. (1997) *J. Cell. Biochem.* **65,** 325–339
21. Haas, A. R., and Tuan, R. S. (2000) *Methods Mol. Biol.* **137,** 383–389
22. Helden, C. H., Miyazono, K., and Dijke, P. (1997) *Nature* **390,** 465–471
23. Massague, J., and Wotton, D. (2000) *EMBO J.* **19,** 1745–1754
24. Iwasaki, S., Iguchi, M., Watanabe, K., Hosono, R., Tsujimoto, M., and Kohno, M. (1999) *J. Biol. Chem.* **274,** 26503–26510
25. Kimura, N., Matsuo, R., Shibuya, H., Nakashima, K., and Taga, T. (2000) *J. Biol. Chem.* **275,** 17647–17652
26. Lee, J. K., Kim, S. H., Lewis, E. C., Azam, T., Reznikov, L. L., and Dinarello, C. A. (2004) *Proc. Natl. Acad. Sci. U. S. A.* **25,** 8815–8820
27. Subbaramaiah, K., Hart, J. C., Norton, L., and Dannenberg, A. J. (2000) *J. Biol. Chem.* **275,** 14838–14845
28. Xia, Z., Dickens, M., Raingeaud, J., Davis, R. J., and Greenberg, M. E. (1995) *Science* **270,** 1326–1331
29. Kawasaki, H., Morioka, T., Shimohara, S., Kimura, J., Hirano, T., Gotoh, Y., and Nishida, E. (1997) *J. Biol. Chem.* **272,** 18518–18521
30. Ghatan, S., Larner, S., Kinoshita, Y., Hetman, M., Patel, L., Xia, Z., Youle, R. J., and Morrison, R. S. (2000) *J. Cell Biol.* **150,** 335–347
31. Zhu, Y., Mao, X. O., Sun, Y., Xia, Z., and Greenberg, D. A. (2002) *J. Biol. Chem.* **277,** 22909–22914
32. Watanabe, H., Caestecker, M. P., and Yamada, Y. (2001) *J. Biol. Chem.* **276,** 14466–14473
33. Lim, Y. B., Kang, S. S., An, W. G., Lee, Y. S., Chun, J. S., and Sonn, J. K. (2003) *J. Cell. Biochem.* **88,** 713–718
34. Zhen, X., Wei, L., Wu, Q., Zhang, Y., and Chen, Q. (2001) *J. Biol. Chem.* **276,** 4879–4885
35. Kronenberg, H. M. (2003) *Nature* **423,** 332–336
36. Olsen, B. R., Reginato, A. M., and Wang, W. (2000) *Annu. Rev. Cell Dev. Biol.* **16,** 191–220
37. Inada, M., Yasui, T., Nomura, S., Miyake, S., Deguchi, K., Himeno, M., Sato, M., Yamagiwa, H., Kimura, T., Yasui, N., Ochi, T., Endo, N., Kitamura, Y., Kishimoto, T., and Komori, T. (1999) *Dev. Dyn.* **214,** 279–290
38. Kim, I. S., Otto, F., Zabel, B., and Mundlos, S. (1999) *Mech. Dev.* **80,** 159–170
39. Takeda, S., Bonnamy, J. P., Owen, M. J., Ducy, P., and Karsenty, G. (2001) *Genes Dev.* **15,** 467–481
40. Yoshida, C. A., Yamamoto, H., Fujita, T., Furuichi, T., Ito, K., Inoue, K., Yamana, K., Zanma, A., Takada, K., Ito, Y., and Komori, T. (2004) *Genes Dev.* **18,** 952–963
41. Zheng, Q., Zhou, G., Morello, R., Chen, Y., Garcia-Rojas, X., and Lee, B. (2003) *J. Cell Biol.* **162,** 833–842
42. Komori, T., Yagi, H., Nomura, S., Yamaguchi, A., Sasaki, K., Deguchi, K., Shimizu, Y., Bronson, R. T., Gao, Y. H., Inada, M., Sato, M., Okamoto, R., Kitamura, Y., Yoshiki, S., and Kishimoto, T. (1997) *Cell* **89,** 755–764
43. Otto, F., Thornell, A. P., Crompton, T., Denzel, A., Gilmour, K. C., Rosewell, I. R., Stamp, G. W., Beddington, R. S., Mundlos, S., Olsen, B. R., Selby, P. B., and Owen, M. J. (1997) *Cell* **89,** 765–771
44. Leboy, P., Grasso-Knight, G., D'Angelo, M., Volk, S. W., Lian, J. V., Drissi, H., Stein, G. S., and Adams, S. L. (2001) *J. Bone Joint Surg. Am.* **83,** Suppl. 1, S15–S22
45. Drissi, M. H., Li, X., Sheu, T. J., Zuscik, M. J., Schwarz, E. M., Puzas, J. E., Rosier, R. N., and O'Keefe, R. J. (2003) *J. Cell. Biochem.* **90,** 1287–1298
46. Mengshol, J. A., Vincenti, M. P., and Brinckerhoff, C. E. (2001) *Nucleic Acids Res.* **29,** 4361–4372
47. Vega, R. B., Matsuda, K., Oh, J., Barbosa, A. C., Yang, X., Meadows, E., McAnally, J., Pomajzi, C., Shelton, J. M., Richardson, J. A., Karsenty, G., and Olson, E. N. (2004) *Cell* **119,** 555–566
48. Park, J. H., Park, B. H., Kim, H. K., Park, T. S., and Baek, H. S. (2002) *Mol. Cell. Endocrinol.* **192,** 197–203
49. Kamiya, N., Jikko, A., Kimata, K., Damsky, C., Shimizu, K., and Watanabe, H. (2002) *J. Bone Miner. Res.* **17,** 1832–1842
50. Lim, Y. B., Kang, S. S., Park, T. K., Lee, Y. S., Chum, J. S., and Sonn, J. K. (2000) *Biochem. Biophys. Res. Commun.* **273,** 609–613
51. Ratisoontorn, C., Seto, M. L., Broughton, K. M., and Cunningham, M. L. (2005) *Bone* **36,** 627–634
52. Sen, A., Lea-Currie, Y. R., Sujkowska, D., Franklin, D. M., Wilkison, W. O., Halvorsen, Y. D., and Gimble, J. M. (2001) *J. Cell. Biochem.* **26,** 312–319
53. Horiki, M., Imamura, T., Okamoto, M., Hayashi, M., Murai, J., Myoui, A., Ochi, T., Miyazono, K., Yoshikawa, H., and Tsumaki, N. (2004) *J. Cell Biol.* **165,** 433–445
54. Lanske, B., Karaplis, A. C., Lee, K., Luz, A., Volkamp, A., Pirro, A., Karperien, M., Defize, L. H., Ho, C., and Mulligan, R. C. (1996) *Science* **273,** 663–666

55. Vorkamp, A., Lee, K., Lanske, B., Segre, G. V., Kronenberg, H. M., and Tabin, C. J. (1996) *Science* **273,** 613–622
56. Minina, E., Kresche, C., Naski, M. C., Ormitz, D. M., and Vorkamp, A. (2002) *Dev. Cell* **3,** 439–449
57. Conlon, R. A., and Herrmann, B. G. (1993) *Methods Enzymol.* **225,** 373–383
58. Lefebvre, V., Zhou, G., Mukhopadhyay, K., Smith, C. N., Zhaoping, Z., Eberspaecher, H., Zhou, X., Sinha, S., Maity, S. N., and de Crombrugghe, B. (1996) *Mol. Cell. Biol.* **16,** 4512–4523
59. Chauchereau, A., Mathieu, M., de Saintignon, J., Ferreira, R., Pritchard, L. L., Mishal, Z., Dejean, A., and Harel-Bellan, A. (2004) *Oncogene* **23,** 8777–8784
60. Ito, K., Hanazawa, T., Tomita, K., Barnes, P. J., and Adcock, I. M. (2004) *Biochem. Biophys. Res. Commun.* **315,** 240–245
61. Schmid, T. M., and Linsenmayer, T. F. (1983) *J. Biol. Chem.* **258,** 9504–9509
62. Gibson, G. J., and Flint, M. H. (1985) *J. Cell Biol.* **101,** 277–284
63. Huang, W., Zhou, X., Lefebvre, V., and de Crombrugghe, B. (2000) *Mol. Cell. Biol.* **20,** 4149–4158
64. Katagiri, T., Yamaguchi, A., Ikeda, T., Yoshiki, S., Wozney, J. M., Rosen, V., Wang, E. A., Tanaka, H., Omura, S., and Suda, T. (1990) *Biochem. Biophys. Res. Commun.* **172,** 295–299
65. Ahrens, M., Ankenbauer, T., Schroder, D., Hollnagel, A., Mayer, H., and Gross, G. (1993) *DNA Cell Biol.* **12,** 871–880
66. Robins, J. C., Akeno, N., Mukherjee, A., Dalal, R. R., Arnow, B. J., Koopman, P., and Clemens, T. L. (2005) *Bone* **37,** 313–322
67. Lefebvre, V., Huang, W., Harley, V. R., Goodfellow, P. N., and de Crombrugghe, B. (1997) *Mol. Cell. Biol.* **17,** 2336–2346
68. Beitner-Johnson, D., Leibold, J., and Millhorn, D. E. (1998) *Biochem. Biophys. Res. Commun.* **242,** 61–66
69. Zehentner, B. K., Dony, C., and Burtscher, H. (1999) *J. Bone Miner. Res.* **14,** 1734–1741
70. Beier, F., and Luvalle, P. (1999) *Biochem. Biophys. Res. Commun.* **262,** 50–54
71. Lefebvre, V., Li, P., and de Crombrugghe, B. (1998) *EMBO J.* **17,** 5718–5733

J Bone Miner Metab (2006) 24:425–433
DOI 10.1007/s00774-006-0718-8

REVIEW ARTICLE

Takanobu Nakase · Hideki Yoshikawa

Potential roles of bone morphogenetic proteins (BMPs) in skeletal repair and regeneration

Received: July 5, 2006 / Accepted: July 20, 2006

Key words bone morphogenetic protein · skeletal repair · regeneration · gene expression · orthopedics

Introduction

Bone morphogenetic protein (BMP) was originally discovered by Urist in 1965 as a bone-inducing substance in an ectopic site [1], and the term "BMP" was first described by Urist and Strates in 1971 [2]. By 1988, molecular clones, as well as the amino-acid sequences of BMP had been characterized from a highly purified preparation obtained from bovine bone [3]. In 1993, murine molecular clones from murine osteosarcoma had also been identified, and they became available for animal experimental systems [4,5] and enabled the performance of various investigations based on molecular technologies. To date, at least 20 members of the BMP family have been identified. In addition to its bone-inducing activity, BMP is now thought to have essential and multifunctional roles in various other organs during morphogenesis. Now, "BMP" should be better recognized as "body morphogenetic protein" [6].

From the viewpoint of clinical applications in orthopedic medicine, several members of the BMP family are attracting considerable attention as promising therapeutic tools for skeletal regeneration and as target molecules for the treatment of skeletal disorders. Previous investigations showed that BMP-2, -4, and -7 stimulated osteogenic and chondrogenic differentiation via BMP receptor (BMPR) types I and II [7–9]. Smad mediates the intracellular signaling of these BMPs [10]. Another BMP, cartilage-derived morphogenetic protein (CDMP)-1 also known as growth and differentiation factor-5 (GDF-5), reportedly shows unique activities, such as the promotion of chondrogenic differentiation and the induction of tendon tissue in vivo [11,12]. Recombinant BMP-2 and -7 proteins have already been in clinical use in the United States and Europe for problematic trauma cases such as open fractures and nonunions [13,14]. The clinical outcomes have been reported as encouraging.

This article reviews the current findings regarding BMP signaling underlying the process of skeletal repair and regeneration. Which BMPs are involved, and in what manner are they involved in the process of bone repair and regeneration? How are BMPs induced in various orthopedic conditions? In some instances, the BMPs play physiological roles, while in other instances, they play pathological roles. The findings will provide a key to understanding the physiological and pathological natures of BMPs and BMP signals in various orthopedic conditions, leading to novel therapeutic formulations aimed at less invasive and more promising treatment of orthopedic injuries and disorders.

Skeletal repair

Fracture repair

Fracture repair involves a number of regenerative events initiated by the breakage of bone tissue. Cells at fracture sites, i.e., periosteum, para-fracture soft tissue, intramedullary canal, and bone cortex, respond to the impact of the fracture. They proliferate and differentiate into cells of osteogenic and chondrogenic lineages, and this is followed by membranous and endochondral ossification, forming a "fracture callus", leading to fracture union [15] (Figs. 1 and 2).

The sequential process of fracture repair is a repetition of embryonic bone development. However, distinct from

T. Nakase (✉)
Department of Orthopaedic Surgery, Hoshigaokakoseinenkin Hospital, 4-8-1 Hoshioka, Hirakata, Osaka 573-8511, Japan
Tel. +81-72-840-2641; Fax +81-72-840-2266
e-mail: tnakase@ff.iij4u.or.jp

H. Yoshikawa
Department of Orthopaedic Surgery, Osaka University Graduate School of Medicine, Suita, Japan

T. Nakase is a recipient of the JSBMR Academic Award 2005.

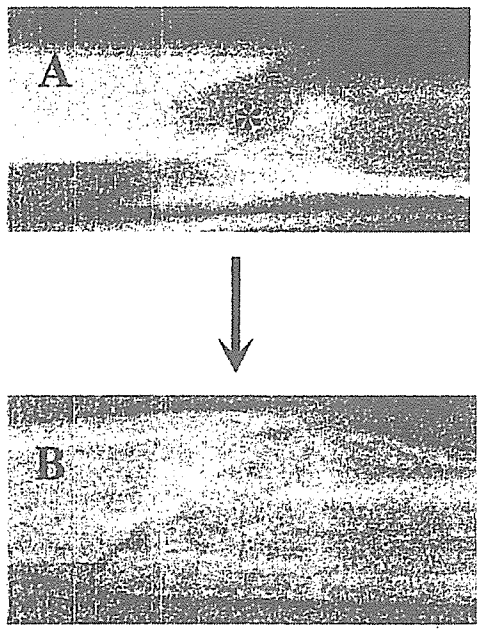

Fig. 1. Radiographic findings, showing repair of human fractured bone. **A** *Asterisk* indicates radiolucent line, showing a fracture. **B** Fractured bones are united by fracture callus

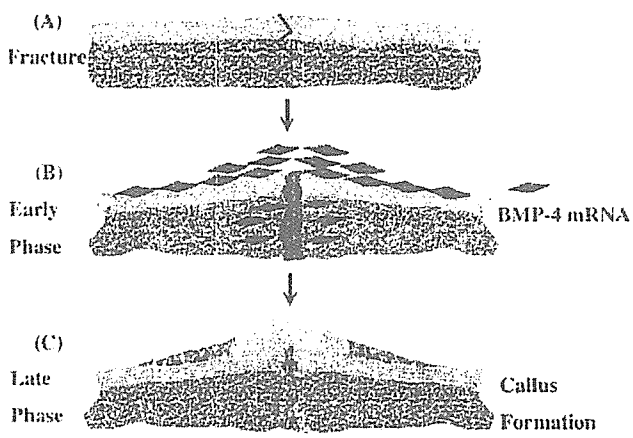

Fig. 2. Localization of bone morphogenetic protein-4 (*BMP-4*) mRNA during the process of fracture repair. **A** Fracture at the mid-shaft of the long bone. **B** Early phase: formation of hematoma at the fracture site, as well as proliferation of immature callus-forming cells in the periosteum, para-fracture soft tissue, and intramedullary cavity. BMP-4 mRNA is induced in the early phase in these immature cells. **C** Late phase: BMP-4 mRNA is no longer detected during the late phase. However, prominent fracture calluses have formed in the periosteal and intramedullary regions

embryogenesis, some kind of stimulus is a prerequisite for the induction of the fracture repair process [15,16]. Our previous in situ hybridization study showed that BMP-4 mRNA was induced in the early phase of fracture repair in the less-differentiated cells at callus-forming sites, such as periosteum, marrow cavity, and surrounding soft tissue. In the later stages, BMP-4 mRNA could no longer be detected (Fig. 2) [15]. These findings have been confirmed by semiquantitative reverse transcription-polymerase chain

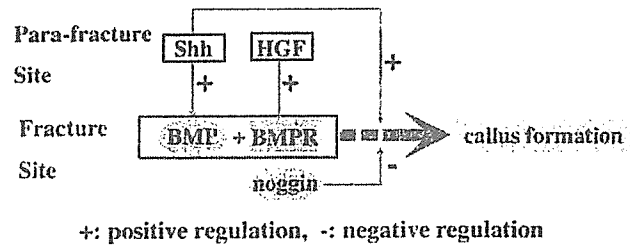

Fig. 3. Hypothetical scheme showing a "BMP network" in the mechanism of fracture repair. BMP and BMP receptor (*BMPR*) induced at the fracture site initiate callus formation. Sonic hedgehog (*Shh*) and hepatocyte growth factor (*HGF*) synthesized at the para-fracture site positively regulate BMP-dependent callus formation, whereas noggin inhibits the effect of BMP on callus formation

reaction (RT-PCR) [15]. Similar findings have been reported in several other studies. On immunohistochemical analysis, using specific antibodies for BMP-2, -4, and osteogenic protein (OP)-1 (BMP-7), these members of the BMP family were shown to be upregulated in the early phase of fracture-healing in immature cells, and continuous expression was observed throughout the healing process [17,18]. In other reports using a rat fracture model, these members of the BMP family were upregulated in the early phase, but such induction was decreased and delayed in older rats [19].

BMP signaling molecules, such as BMPR types IA, IB, and II have also been identified in locations similar to those for BMPs during fracture healing [17,20]. The BMPs and BMP signaling components are localized at callus-forming sites, suggesting the key roles of BMPs in fracture repair, and raising the possibility of their use as target or therapeutic molecules for fracture treatment. For example, *BMP-4* gene transfer into the periosteum in the early phase dramatically enhanced fracture healing in a rat model [21].

In addition to BMP itself, other BMP-related factors have been identified during fracture healing. Sonic hedgehog (Shh), a stimulator of BMP-dependent chondrogenic and osteoblastic differentiation [22,23], has been identified at the para-fracture site in the early phase, and may promote BMP-induced callus formation [24]. Hepatocyte growth factor (HGF) is located at the para-fracture site, with its receptor c-Met [25]. In vitro studies have shown that HGF upregulates BMPR expression in mesenchymal cells, and may contribute to BMP-dependent callus formation [25]. In addition to these positive regulators of BMP signaling, noggin is reportedly co-localized with BMP-4 throughout the healing process [26]. Overexpression of noggin reportedly inhibits BMP-dependent chondrogenesis [26], and noggin may negatively regulate BMP-induced callus formation during fracture repair. These current findings suggest that the process of fracture repair is regulated by various BMP-related factors located in distinct areas, forming a "BMP network" (Fig. 3).

Although most investigations have been performed using animal models, several current studies have shown the actual expression of BMPs in human situations. BMP-2, -4, and -7, as well as BMPR types IA, IB, II, and Smad 1, have

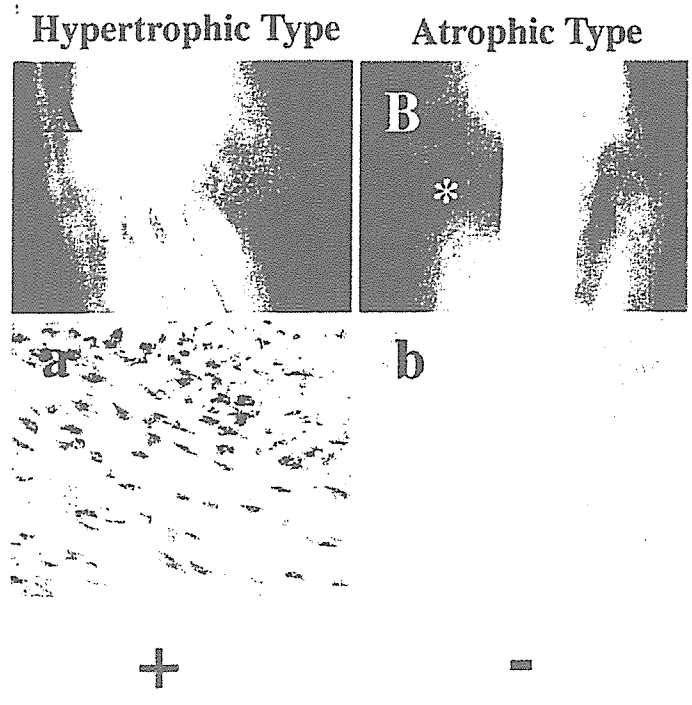

Fig. 4. Expression and localization of BMP-2 and -4 mRNA in surgical specimens of hypertrophic (**A** and **a**) and atrophic (**B** and **b**) callus. **A** and **B** Radiographic findings; **a** and **b** in situ hybridization, using BMP-2-specific probes. BMP-2 (**a** and **b**) and BMP-4 (data not shown) mRNAs are localized in immature fibroblastic cells in hypertrophic callus (a; *asterisk* area in A), but not in atrophic callus (b; *asterisk* area in B). These findings were confirmed by reverse transcription-polymerase chain reaction (RT-PCR)

been detected in human fracture callus specimens [28,29]. However, the ubiquitous expression of these BMP family members did not suggest specific roles of the BMP family members in fracture healing in human situations. In our current unpublished observations, BMP-2 and BMP-4 mRNA and proteins were identified in tissue from hypertrophic (viable) nonunion callus, but they were not identified in tissue from atrophic (nonviable) nonunion callus (Fig. 4); these findings suggest possible roles of BMPs in callus formation in human situations.

To summarize, BMPs seem to play crucial roles in the events of fracture healing. Several BMP family members, such as BMP-2, -4, and -7, will certainly serve as therapeutic molecules in fracture treatment. The mechanisms of BMP induction in the early phase of fracture repair might provide a key to solving the mechanism of bone regeneration. The series of current findings regarding the roles of BMP and related factors in fracture repair will provide a key for the formulation of therapeutic strategies for less invasive and more definitive fracture treatment.

Tendon repair

BMPs are not only involved in bone repair but also in tendon repair. The BMPs involved in tendon repair are GDF-5 (CDMP-1/BMP-14), GDF-6 (CDMP-2/BMP-13), and GDF-7 (CDMP-3/BMP-12). These molecules induce tendon formation at ectopic sites in rats [12].

CDMP-1 has been identified in tendon tissue undergoing repair in the shoulder joint (rotator cuff) in human specimens [30]. Upregulated localization of CDMP-1 at the torn site has been observed. Both CDMP-1 mRNA and the protein were predominantly localized in cells at the torn edge and bursa side (Fig. 5). Various animal studies using gene knockout mice have revealed the potential roles of these molecules in tendon repair [31,32] and they are becoming promising therapeutic agents for tendon surgery [33].

Mechanical stress and skeletal regeneration

Induction of the *BMP* gene is a particularly important focus of interest in orthopedic medicine, because it holds a key to solving the central mechanism of skeletal regeneration. Mechanical stress is one of the crucial factors stimulating skeletal regeneration, and our current findings suggest that mechanical stress may induce BMP expression.

Distraction osteogenesis

The effect of mechanical stretching on skeletal regeneration has been dramatically corroborated by such surgical procedures as distraction osteogenesis, a principle first introduced by Ilizarov [34]. Gradual distraction between the bone fragments after osteotomy induces bone regeneration within the distraction gap (Fig. 6). This regenerative effect has been characterized by the gene expression of *BMP-2* and *BMP-4* in the lengthened callus [35]. BMP-2 and -4 mRNAs were upregulated just after the osteotomy, as they are in fracture repair. However, after the beginning of the distraction, the gene expressions of *BMP-2* and *BMP-4* were shown to have increased up to tenfold by upregulation. In contrast, the level of GDF-5 and BMP-6 mRNA did not seem to be affected by the distraction stress (Fig. 7) [35]. These findings indicate the positive effect of

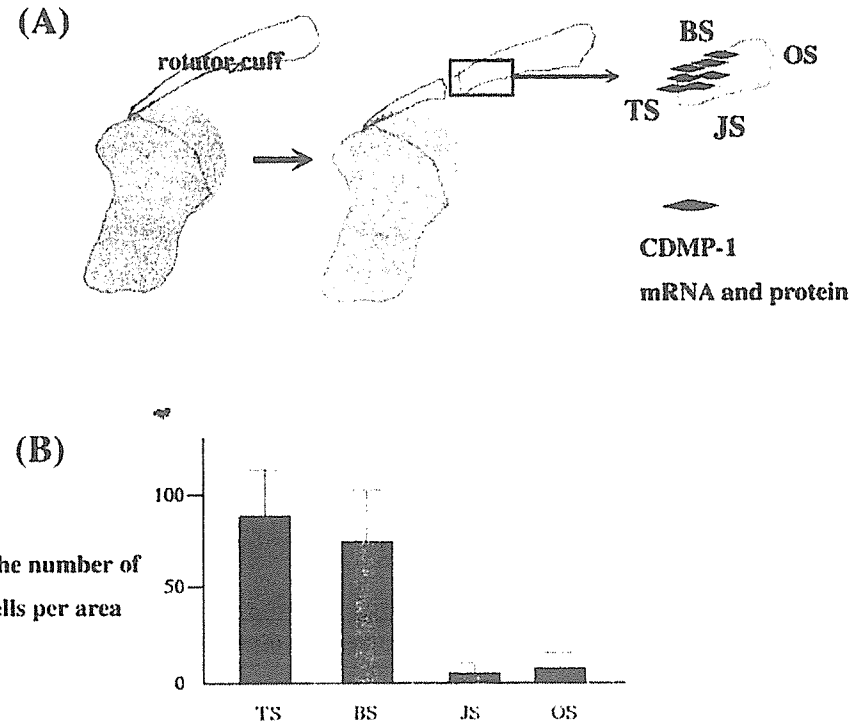

Fig. 5. **A** Localization of cartilage-derived morphogenetic protein-1 (*CDMP-1*) mRNA and protein in torn rotator cuff. CDMP-1 is predominantly localized in cells at the torn edge and bursa side. *TS*, Torn edge side; *BS*, bursa side; *JS*, joint side; *OS*, opposite side to torn edge. **B** Cell count analysis revealed a marked increase in CDMP-1-positive cells in the torn edge and bursa side

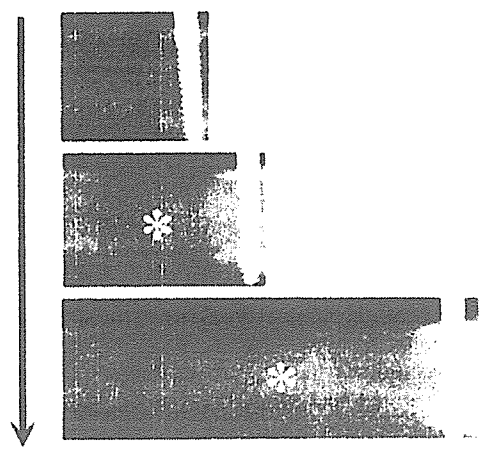

Fig. 6. Radiographic findings showing gradual distraction osteogenesis. Regenerative bone formation is seen in the distraction gap (*asterisk*)

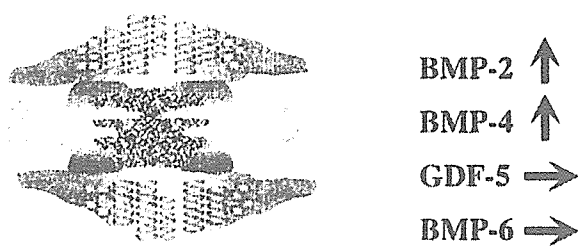

Fig. 7. Schematic illustration, showing lengthening callus formed in the distraction gap. During the distraction phase, BMP-2 and -4 mRNAs are induced, whereas the expression of growth and differentiation factor-5 (*GDF-5*) and BMP-6 mRNAs is not affected by distraction stress

mechanical tension stress on the induction of gene the expression of *BMP-2* and *BMP-4*.

Mechanical overload-induced spondylosis

Mechanical overload sometimes induces bone regeneration. This phenomenon often occurs at the bone-cartilage-tendon junction. One example of this phenomenon occurs at the disco-vertebral junction in some spinal regions [36] (Fig. 8). In a mouse model of spondylosis induced by resection of the posterior components of the cervical spine, prominent and rapid growth of an osseous spur in the anterior portion of the affected spine was seen [37]. Such a phenomenon is similar to that observed in human spondylosis, in which chronological histological observations show a process of bone regeneration resembling endochondral ossification. Molecular mechanisms underlying the sequential process of spondylosis in the mouse model have been investigated by in situ hybridization, using specific cDNAs for BMP-related factors [38]. In the early stage, cells in the anterior margin of the disc beside the attachment of the spinal ligament (annulus-ligament complex; ALC) proliferate, showing metaplasia, into round chondrocyte-like cells. BMP-4 mRNA is localized predominantly in cells in the anterior margin of the disc (ALC), together with ALK-6 (BMPR IB and II) mRNA. GDF-5 and BMP-6 mRNAs are not detected at this stage. In the late stage, fibroblastic cells are almost totally replaced by mature chondrocytes. Enlargement of cartilaginous tissues, together with osteophyte tissue, is observed in the anterior margin of the disc. Cells positive for *BMP-4* decrease, whereas GDF 5 and BMP-6 mRNAs are localized in cells undergoing chondrogenesis.

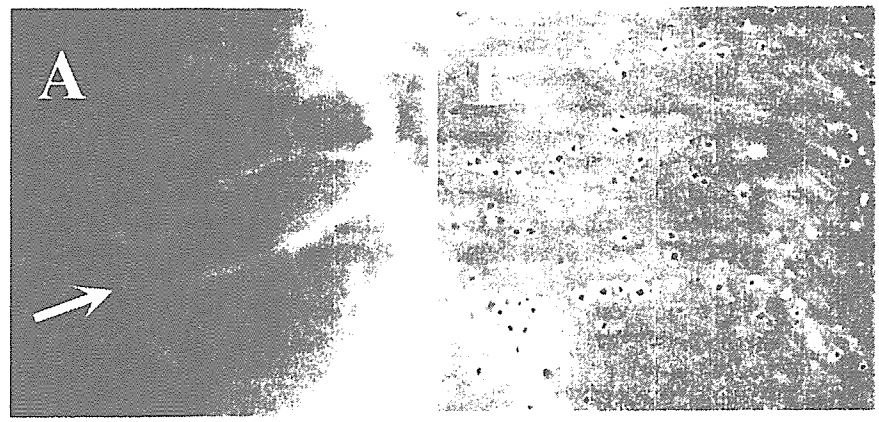

Fig. 8. A Radiographic findings showing osteophyte formation (*arrow*) in human cervical spondylosis. B Histological findings showing round chondrocyte-like cells in the anterior margins of the disco-vertebral junction in human spondylosis. Hematoxylin and Eosin Staining, ×100

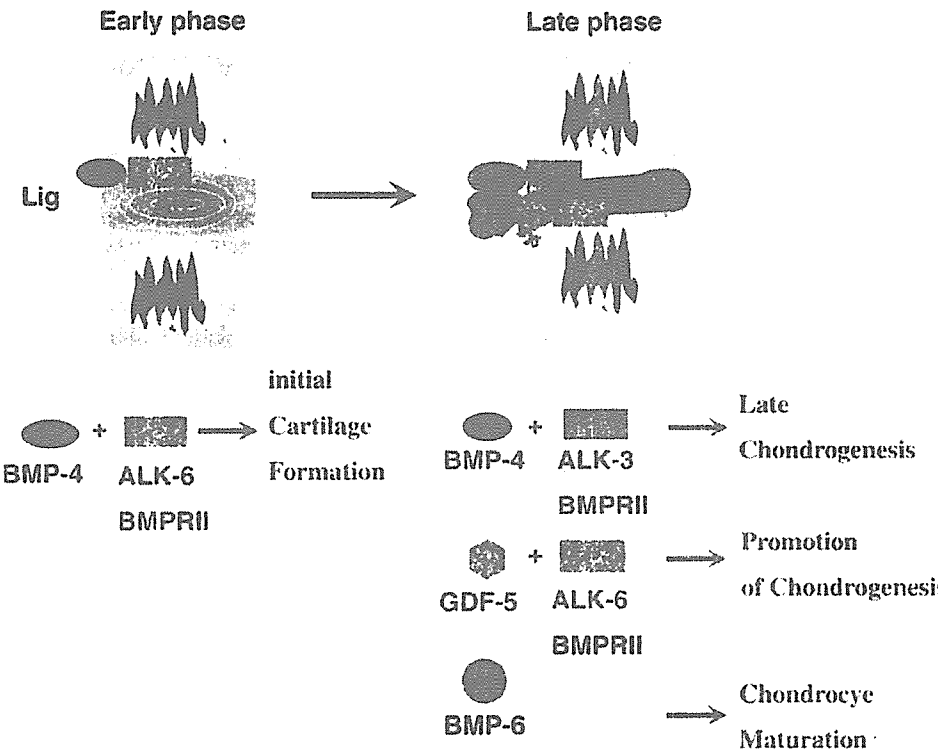

Fig. 9. Proposed scheme of the involvement of BMP signals underlying spondylosis produced in a mouse model. BMP-4 mRNA is induced at the anterior annulus-ligament complex, and ALK-6 (BMPR IB) and BMPR II mediate BMP-4-dependent initial chondrogenesis. In the late phase, BMP-4 regulates late chondrogenesis via ALK-3 (BMPR IA)/BMPR II, and GDF-5 promotes chondrogenesis via ALK-6/BMPR II. BMP-6 mRNA is activated and BMP-6 possibly stimulates chondrocyte maturation. (*Lig*, ligament; *Vb*, vertebral body; *An*, annulus fibrosus

ALK-3 (BMPR IA) mRNA begins to appear at this stage, together with the ALK-6 and BMPR II mRNA that is already present [38].

Together with the reported roles of these molecules in endochondral ossification, the molecular mechanisms underlying the above mouse model [38] are thought to be as follows (Fig. 9): BMP-4/ALK-6 is activated, most likely by the mechanical stimuli, and regulates initial chondrogenesis at the ALC. BMP-4/ALK3 and GDF-5/ALK-6 promote cartilage formation and enlargement of the cartilaginous matrix [38]. Such BMP signaling may act as a mediator in the process of mechanical overload-induced bone regeneration.

Pathological skeletal disorders

Skeletal regeneration sometimes leads to pathological conditions in orthopedic medicine. Newly generated osseous tissues cause problematic phenomena, such as neurovascular compression/irritation, joint contractures and pain. Current reports suggest the involvement of BMPs in such conditions and possible roles of BMPs as therapeutic targets in skeletal disorders.

Ossification of the spinal ligament

Ossification of the spinal ligament or ligamentum flavum is a pathologic condition leading to compression of the spinal